Insect Systematics and Diversity, 2026, **10**(1), ixaf060
DOI: https://doi.org/10.1093/isd/ixaf060
Research

ENTOMOLOGICAL SOCIETY OF AMERICA
SHARING INSECT SCIENCE GLOBALLY

OXFORD

Molecular Phylogenetics, Phylogenomics, and Phylogeography

Ecological, morphological, and molecular diversification in a clade of Melanesian *Ethmostigmus* centipedes (Chilopoda: Scolopendromorpha), with the description of 2 new species

Valter Weijola*[,1], Gregory D. Edgecombe[2], Bulisa Iova[3], Carlos A. Martínez-Muñoz[4], Conny Sjöqvist[5], and Varpu Vahtera[1]

[1]Zoological Museum, Biodiversity Unit, University of Turku, Finland
[2]The Natural History Museum, London, UK
[3]Papua New Guinea National Museum and Art Gallery, National Capital District, Papua New Guinea
[4]Senckenberg Research Institute and Museum, Frankfurt-am-Main, Germany
[5]Environmental and Marine Biology, Åbo Akademi University, Åbo, Finland

*Corresponding author. Zoological Museum, Biodiversity Unit, FI-20014 University of Turku, Finland (Email: vsawei@utu.fi).

Subject Editor: Rodrigo Monjaraz-Ruedas

Populations of the large scolopendrid centipede *Ethmostigmus* Pocock 1898, from five islands of the Bismarck volcanic arc between New Guinea and New Britain comprise a monophyletic group within which three species can be identified based on each forming a strongly supported clade based on concatenated sequence data for three genes, diagnostic morphological characters, and ecology. Two species occurred in sympatry on four of the islands, and all three species are sympatric on the island of Umboi. The two best-sampled and most widely geographically overlapping species are each other's closest relative, one of them only collected from the ground and the other from trees, a pattern consistent across all islands on which they occur. The tree-dwelling species, *Ethmostigmus arboreus* **sp. nov.**, is distinguished from the ground species, *Ethmostigmus platycephalus* (Newport, 1845), by having longer legs. This pair's sister species, *Ethmostigmus krausi* **sp. nov.** from the islands of Umboi and Sakar, is readily distinguished by rugose and coarsely granulate tergal sculpture. This radiation exhibits ecological partitioning at a spatial scale that has not previously been documented in centipedes.

Keywords: Scolopendridae, Otostigminae, *Ethmostigmus*, habitat partitioning, ecomorphology

Introduction

Islands and island archipelagos have inspired the study of evolutionary processes and speciation ever since the works of Darwin (1859) and Wallace (1880). The study of insular faunal communities has formed the basis for the conceptualization of speciation processes such as adaptive radiation (Darwin 1845), character displacement (Brown and Wilson 1956), and the taxon cycle (Wilson 1961). Islands have been particularly useful for understanding competitive interactions (or the absence of them) due to their depauperate and disharmonic species assemblages often lacking entire ecological guilds that are present on mainland areas (eg most mammals, amphibians). The reduced competition faced by island colonizers provides novel ecological opportunities, which can lead to niche expansion, niche shift, and/or density compensation (higher population densities) (Diamond 1970). On an evolutionary timescale, these ecological shifts can manifest themselves in morphological adaptations to new habitats and eventually the formation of new species.

The oceanic barrier between islands separates the founder population from its source and establishes opportunities for allopatric speciation. In an island archipelago, newly formed species may then colonize additional islands, or return to the ancestral species' source region, and come into competition with close relatives. These competitive interactions can result in further ecological and morphological segregation and be the start of the so-called "archipelago mode of adaptive radiation" (Grant and Grant 2008, Price 2008). Insular evolutionary processes in arthropods specifically have been reviewed by several authors (eg Gillespie and Roderick 2002, Pérez-Delgado et al. 2022).

Received: 1 September 2025; **Revised:** 27 November 2025; **Accepted:** 9 December 2025

Version of Record, first published online [29th January], with fixed content and layout in compliance with Art. 8.1.3.2 ICZN.

Melanesia—a region spanning from New Guinea to Fiji—is composed of around 2000 islands of varying ages, sizes, elevations, isolation, and geological origins. In relation to land area, it holds an exceptionally high level of biodiversity, particularly for some taxonomic groups (Cámara-Leret et al. 2020, Oliver *et al.* 2022, Slavenko et al. 2023, Oliver et al. 2024). The level of regional/local endemism is also high in many taxa (Duffels 1986, Polhemus *et al.* 2004, Oliver *et al.* 2022). Altogether, this makes it an intriguing area for the study of evolutionary processes (Wilson 1961, Diamond *et al.* 1989).

The Bismarck volcanic arc includes a string of cinder-cone islands of Quaternary origin located to the west of New Britain along the northern coast of New Guinea (Fig. 1) (Johnson et al. 1972, Robinson and Jaques 1978). The largest of these is Umboi at 880 km^2, but most others are much smaller. Compared to New Guinea and New Britain, they have depauperate species communities, and only a few taxa are presumed to be endemic (Kraus and Weijola 2019, Kraus *et al.* 2023, Kraus *et al.* 2024).

The chilopod order Scolopendromorpha dates at least to the Late Carboniferous and contains 27 extant genera and over 700 species (Edgecombe 2011, Edgecombe and Bonato 2011, Schileyko *et al.* 2020). The largest family within this order, Scolopendridae Leach (1814), includes some 400 species divided among 19 genera. One of these, the Old World genus *Ethmostigmus* Pocock (1898), forms a modest radiation of 18 recognized species (Joshi and Edgecombe 2018), with its highest diversity being in India, the New Guinea region, and Australia, with little species diversity in the westernmost part of its range, across tropical Africa. *Ethmostigmus*, like many other scolopendromorph genera, is morphologically conservative in some parts of its geographic range (eg Peninsular India: Joshi and Edgecombe 2018), whereas in other regions, such as Australia, it exhibits considerable variation among species (Koch 1983) and captures most of the size variation shown in the genus as a whole (Edgecombe and Bonato 2011).

Our understanding of ecology and habitat use of scolopendrids is mostly known in only a very broad sense (Voigtländer 2011). Within *Ethmostigmus*, phenology and life-history data are best known from Nigerian populations of the widespread African species *Ethmostigmus trigonopodus* (Lewis 1972). A few partly amphibious scolopendrid species have been recorded (eg Siriwut *et al.* 2016, Tsukamoto *et al.* 2021), and some others have been documented to lead a partly arboreal lifestyle (Kronmüller 2009, Hodges and Goodyear 2021). Few studies have been made on niche partitioning among closely related sympatric species (eg different species or relative abundances are noted in communities from low- and high-canopy rainforest epiphytes; Phillips *et al.* 2020). Although data on species distributions are in many cases fragmentary, available data suggest that multiple large species of *Ethmostigmus* may occur in sympatry in regions such as Wallacea and Melanesia, but if and how these differ ecologically is unknown (Schileyko and Stoev 2016, Joshi and Edgecombe 2018, Chilobase [accessed November 2025]).

Based on transcriptomics, phylogenetic relationships within Scolopendromorpha are well known at the deepest (interfamilial) levels (Benavides *et al.* 2021), and multi-locus Sanger data provide reasonable resolution at shallower nodes (Vahtera *et al.* 2012, 2013). There are, however, only a few detailed phylogenetic studies focused on specific genera or geographical regions, such as Melanesian *Ethmostigmus*. Exceptions include an integrative taxonomic revision of *Scolopendra* in Southeast Asia (Siriwut *et al.* 2015, 2016) and for scolopendrids of Peninsular India (Joshi *et al.* 2020), including *Ethmostigmus* (Joshi and Edgecombe 2018, 2019).

During herpetological surveys of several islands (Crown, Tolokiwa, Umboi, and Sakar) in the Bismarck volcanic arc in Papua New Guinea, 2 of the authors (V.W. and B.I.) noted an unusually high abundance of 3 different large-sized *Ethmostigmus* spp. (Fig. 2). One species was collected in pit-fall traps installed for ground-dwelling lizards and blind snakes, while a second species was hand-collected from trees during nocturnal surveys of arboreal geckos. A third species was restricted to just 2 of the islands (Umboi and Sakar), and the limited number

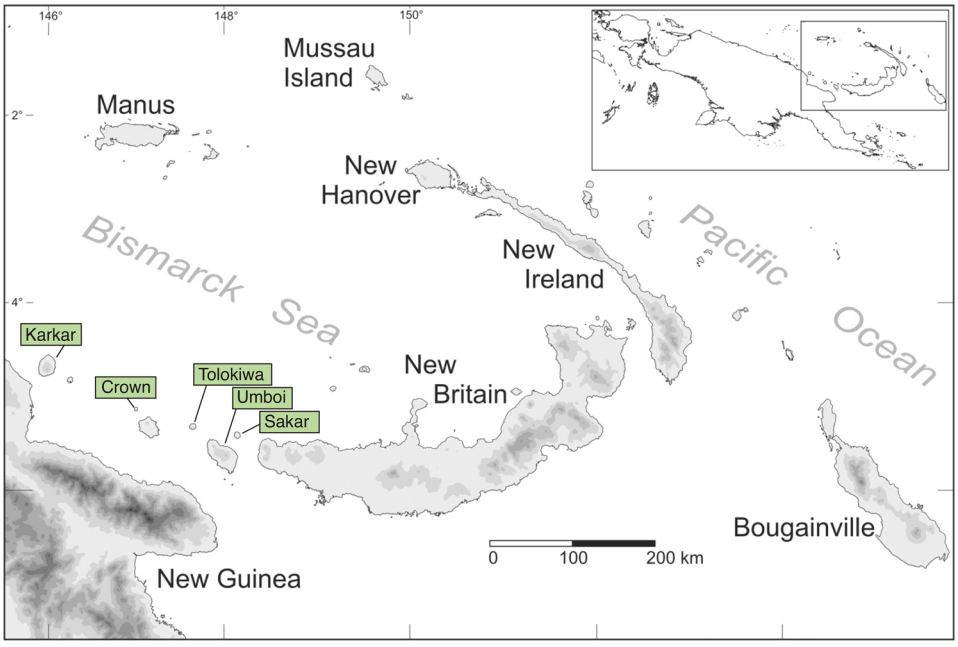

Fig. 1. Map of islands in the Bismarck volcanic arc from which *Ethmostigmus* specimens were collected.

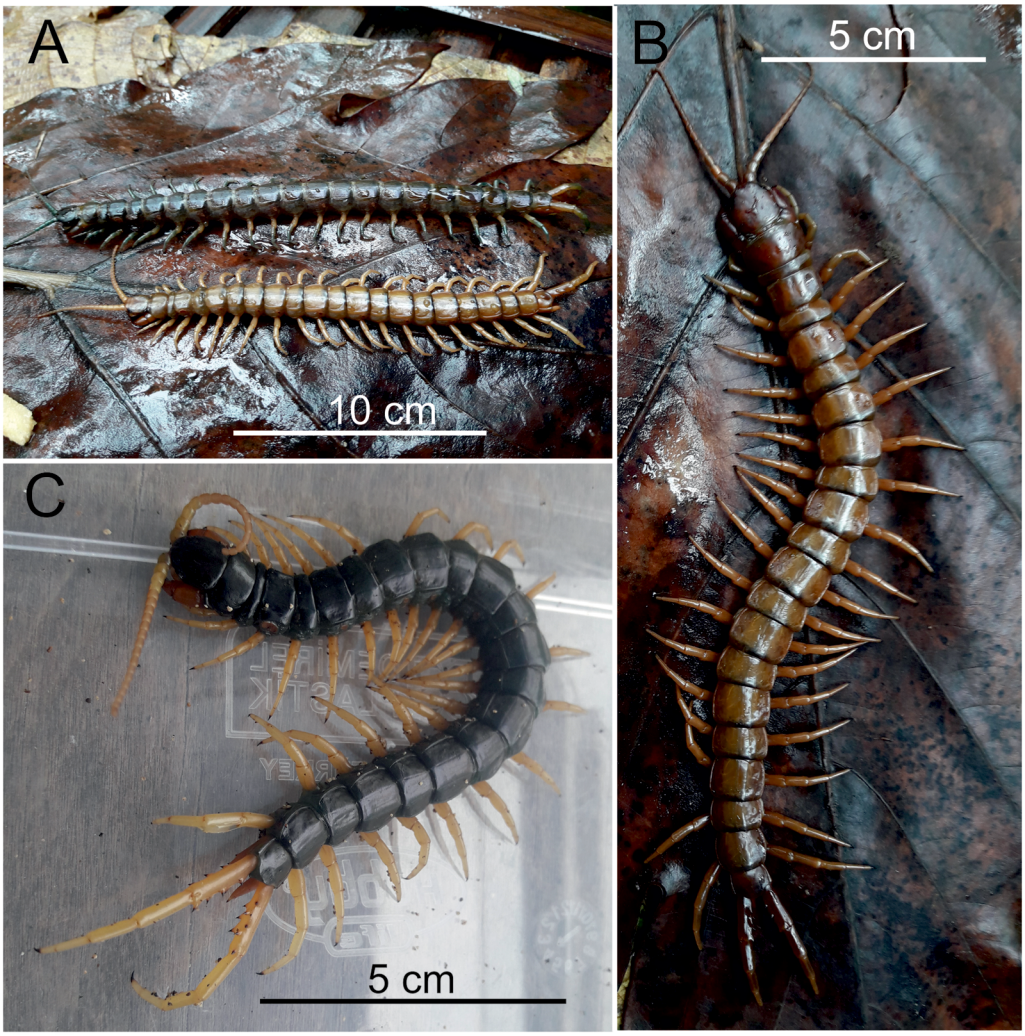

Fig. 2. Habitus photographs of *Ethmostigmus* specimens from the Bismarck volcanic arc. A) *E. platycephalus* (Newport 1845) (top) and *E. arboreus* sp. nov. (bottom) from Crown; B) *E. arboreus* from Crown; and C) *E. krausi* sp. nov. from Umboi.

of observations failed to resolve whether that species displays a similarly specialized use of habitat.

In order to gain an understanding of the evolutionary history resulting in this ecological diversification, we reconstructed phylogenetic relationships and analyzed differences in limb length and article proportions between the 3 species.

Materials and Methods

Field Sampling

Specimens were collected between February and May 2018 on the islands of Karkar, Crown, Tolokiwa, Umboi, and Sakar (Fig. 1) in Madang and Morobe Provinces in Papua New Guinea. Centipedes were caught either as bycatch in bucket traps connected with plastic drift fences set up to catch leaf-litter lizards and snakes or by actively catching them from tree trunks at night, or from inside rotten logs or the leaf axils of pandanus trees during day time. On Umboi and Sakar, several specimens were also brought to us by locals. To preserve specimens and their DNA, all samples were stored in 96% EtOH before being deposited at the Zoological Museum of the University of Turku (ZMUT).

Taxonomy

Standard meristic data used in otostigmine species-level taxonomy were tabulated for all specimens collected. These include number of antennal articles; number of glabrous articles; legs that bear spurs on the prefemur, femur, tibia, and tarsus; number of tarsal spurs on each leg; numbers of apical, subapical dorsal, and lateral spines on the coxopleural process; the first tergite with complete margination; and number of spines in 3 rows on the ultimate leg prefemur. Species descriptions follow a format used in recent work on *Ethmostigmus* in India (Joshi and Edgecombe 2018).

Type specimens of several named species of *Ethmostigmus* from Melanesia and Southeast Asia were examined, supplemented with published descriptions and illustrations. Species are identified in our sample based on monophyly and strong node support in molecular phylogenetic trees, pairwise distance from other putative species, results of 2 different species delimitation methods, and diagnostic morphological characters; 2 of 3 such clades also present distinct ecologies. We name 2 of these clusters as new species and assign 1 to a species identified from New Guinea in the most recent morphology-based taxonomy from the region (Schileyko and Stoev 2016).

Because differences in relative length of the legs were apparent in our sample, these were measured and analyzed as described in the following section.

Morphometric Analysis

There are no standardized procedures for analyzing limb and article morphology in centipedes. In this study, measurements were restricted to 1 anterior trunk leg from leg pair 6 and 1 posterior leg from leg pair 20 of each specimen. These are referred to as LP6 and LP20, respectively. The length of the strongly sclerotized cephalic plate was used as a proxy for specimen size and is referred to as HL ("head length") in the remainder of the text. Legs in LP6 and LP20 were first removed and then photographed and measured using a CANON 7D mark 2 digital camera attached to an OLYMPUS SZX16 stereomicroscope, with QuickPHOTO MICRO 3.1 software. Measurements were taken for each leg article (prefemur, femur, tibia, tarsus 1, tarsus 2) to the nearest 0.01 mm. The claw length was not included in the analyses due to the difficulty in retrieving reliable measurements. Sample numbers for the respective species were 10, 22, and 25 (for morphometric data, see Supplementary File S1).

As the use of ratios to correct morphometric values for body size has been criticized by Humphries *et al.* (1981), we followed their recommendation to also evaluate differences in the lengths of articles using ordination analysis (Linear Discriminant Analysis [LDA] in this case) on log-adjusted article values. To confirm that the proportions of articles scaled isometrically with HL, we analyzed the correlation of logarithmic values of HL in relation to the lengths of articles (prefemur, femur, tibia, tarsus 1, and tarsus 2) in LP6 and LP20 using the "stat_cor" function integrated to the "ggplot"-package (v3.4.3; Wickham 2016) in R (R Core Team 2021) and RStudio (RStudio Team 2021). Isometry proved to be a reasonable assumption based on our initial analyses (Supplementary File S2). To detect potential differences among species between the total leg length of LP6 and LP20 and the lengths of the separate articles, we conducted an analysis of covariance (ANCOVA). For this, HL was used as a covariate to control for the size of the specimen as suggested in Foster *et al.* (2018). An ANCOVA is a technique used to assess the impact of 1 or more independent variables on a dependent variable while controlling for the influence of 1 or more covariates. We concluded that an ANCOVA is a suitable method for testing our hypothesis, as it combines elements of both analysis of variance and regression analysis, making it a powerful tool for examining group differences while accounting for the effects of continuous covariates. We also formally tested if the use of HL as a covariate was appropriate in this case by comparing the adjusted R-square values from confounded (excluding the covariate, HL) vs. controlled models (including HL). The controlled model resulted in higher adjusted R-squared values for all articles, suggesting the use of a covariate in this case was required to obtain statistically sound results.

Each dependent variable (prefemur, femur, tibia, tarsus 1, tarsus 2, and total leg length) was then tested in the ANCOVA model, including HL as the covariate to remove the effect of body size from the studied variables. All models included "Species" ("Arboreal," "Granulated," "Ground") as the independent variable. The homoscedasticity and normality of residuals were assessed prior to conducting the analyses of variance using Levene's test from the "car" package (Fox and Weisberg 2019) and Shapiro–Wilk's test from the "stats" package (R Core Team 2021), respectively. Potential outliers were removed (1 data point in any case) from the data sets, if necessary, to fulfill the technical requirements for analyses of variance. Tukey's post hoc tests ("multicomp-package") (v1.4-25; Hothorn *et al.* 2008) were used to analyze pairwise differences (between species) of articles. As recommended by Humphries *et al.* (1981), an ordination technique was used to further examine the morphological differences between the 3 species. A LDA was used to maximize separation between species while minimizing within-species variance. The LDA analysis was conducted on log-adjusted articles using R and R Studio. The dataset was pre-processed to meet the assumptions of LDA, including normality and homoscedasticity.

Molecular Methods

Samples were stored in 96% EtOH. Total DNA was extracted from legs using a NucleoSpinTissue kit (Macherey-Nagel), applying the standard protocol for human or animal and cultured cells, incubating samples overnight. Mitochondrial 16S rRNA and mitochondrial protein-coding cytochrome *c* oxidase subunit I (COI) were amplified using the primer pairs 16Sa/16Sb (Xiong and Kocher 1991, Edgecombe *et al.* 2002) and LCO1490/HCO2198 (Folmer *et al.* 1994), respectively. In addition, the nuclear 28S rRNA fragment was amplified with the primer pair 28Sa/28Sb (Whiting *et al.* 1997). All primers had a universal tail (T7Promoter/T3) attached to them.

Polymerase chain reaction (PCR) amplifications were performed using MyTaqTM HS Red Mix in a total volume of 23 µl. Each reaction contained 7.5 µl of MQ, 12.5 µl of MyTaq HS Red Mix, 0.5 µl of each primer (10 µM), and 2 µl of DNA template. Initial PCR denaturation occurred at 95 °C for 1 min; all following denaturation steps occurred at 95 °C for 15 s. Annealing occurred for 15 s at 44 °C for 16S and COI and at 49 °C for 28S, followed by extension at 72 °C for 10 s, repeated for 35 cycles. A negative control was included in each run. PCR products were electrophoresed on 1% agarose gel with Midori Green Advanced DNA Stain (Nippon Genetics) and purified with A'SAP PCR clean-up kit (Arctic-Zymes). Sequencing was performed by Macrogen Europe. Chromatograms were visualized and assembled with Sequencher ver. 5 (Gene Codes Corporation, Ann Arbor, MI). All new sequences are deposited in GenBank (Table 1).

Molecular Phylogenetic Analysis

Multiple sequence alignments were first produced in MAFFT7 online service (Kuraku *et al.* 2013, Katoh *et al.* 2019) and then trimmed in Mesquite v 3.10 (Maddison and Maddison 2019).

The 3 separate gene sequences were concatenated with SequenceMatrix (Vaidya *et al.* 2011) for the phylogenetic analyses. The final molecular matrix including all 3 genes (COI, 16S, 28S) consisted of 1,352 characters and 82 taxa (consisting of 54 ingroup and 28 outgroup taxa).

Phylogenetic analyses were conducted using parsimony and maximum likelihood as optimality criteria. For the parsimony analysis, TNT v. 1.5 (Goloboff and Catalano 2016) was used, treating gaps as missing data. The parsimony search strategy consisted of 100 replications and 10 rounds of both ratchet and tree drifting followed by tree fusing (Goloboff 1999). The command xmult was executed until

Table 1. Specimens used for molecular study and their GenBank accession numbers. Novel specimens sequenced in this study are in bold.

Species	Specimen code	Island	Country	COI	16S	28S	
***Ethmostigmus arboreus* sp. nov.**	ZMUT.AA11196	Tolokiwa	PNG	–	**PV464168**	**PV464201**	
***E. arboreus* sp. nov.**	ZMUT.AA11187	Tolokiwa	PNG	–	**PV464172**	**PV464210**	
***E. arboreus* sp. nov.**	ZMUT.AA11195	Tolokiwa	PNG	–	**PV464175**	**PV464215**	
***E. arboreus* sp. nov.**	ZMUT.AA11181	Tolokiwa	PNG	–	**PV464179**	**PV464216**	
***E. arboreus* sp. nov.**	ZMUT.AA11193	Tolokiwa	PNG	–	**PV464173**	**PV464202**	
***E. arboreus* sp. nov.**	ZMUT.AA11194	Tolokiwa	PNG	–	**PV464174**	**PV464203**	
***E. arboreus* sp. nov.**	ZMUT.AA11179	Sakar	PNG	**PV466628**	–	**PV464219**	
***E. arboreus* sp. nov.**	ZMUT.AA11190	Sakar	PNG	–	**PV464178**	**PV464204**	
***E. arboreus* sp. nov.**	ZMUT.AA11188	Sakar	PNG	**PV466626**	**PV464176**	**PV464211**	
***E. arboreus* sp. nov.**	ZMUT.AA11182	Sakar	PNG	**PV466635**	–	**PV464213**	
***E. arboreus* sp. nov.**	ZMUT.AA11189	Sakar	PNG	**PV466629**	**PV464180**	**PV464205**	
***E. arboreus* sp. nov.**	ZMUT.AA11192	Sakar	PNG	**PV466630**	**PV464165**	**PV464206**	
***E. arboreus* sp. nov.**	ZMUT.AA11191	Sakar	PNG	**PV466627**	**PV464177**	**PV464208**	
***E. arboreus* sp. nov.**	ZMUT.AA11186	Umboi	PNG	**PV466631**	**PV464166**	**PV464200**	
***E. arboreus* sp. nov.**	ZMUT.AA11178	Umboi	PNG	–	**PV464169**	**PV464217**	
***E. arboreus* sp. nov.**	ZMUT.AA11184	Umboi	PNG	**PV466632**	**PV464171**	**PV464207**	
***E. arboreus* sp. nov.**	ZMUT.AA11185	Umboi	PNG	**PV466633**	–	**PV464214**	
***E. arboreus* sp. nov.**	ZMUT.AA11183	Umboi	PNG	**PV466634**	**PV464170**	**PV464209**	
***E. arboreus* sp. nov.**	ZMUT.TYPE964	Crown	PNG	**PV466624**	–	**PV464220**	
***E. arboreus* sp. nov.**	ZMUT.TYPE966	Crown	PNG	–	**PV464167**	**PV464218**	
***E. arboreus* sp. nov.**	ZMUT.TYPE965	Crown	PNG	**PV466625**	–	**PV464212**	
***E. krausi* sp. nov.**	ZMUT.TYPE968	Umboi	PNG	**PV466623**	**PV464162**	**PV464252**	
***E. krausi* sp. nov.**	ZMUT.TYPE969	Umboi	PNG	–	**PV464163**	**PV464250**	
***E. krausi* sp. nov.**	ZMUT.TYPE970	Umboi	PNG	–	**PV464159**	**PV464248**	
***E. krausi* sp. nov.**	ZMUT.TYPE971	Umboi	PNG	–	**PV464160**	**PV464251**	
***E. krausi* sp. nov.**	ZMUT.TYPE973	Umboi	PNG	–	**PV464161**	–	
***E. krausi* sp. nov.**	ZMUT.TYPE967	Sakar	PNG	–	**PV464164**	**PV464249**	
E. platycephalus	ZMUT.AA11198	Karkar	PNG	**PV466636**	**PV464181**	**PV464225**	
E. platycephalus	ZMUT.AA11197	Karkar	PNG	–	**PV464182**	**PV464222**	
E. platycephalus	ZMUT.AA11199	Crown	PNG	–	**PV464186**	**PV464226**	
E. platycephalus	ZMUT.AA11209	Crown	PNG	**PV466645**	**PV464187**	**PV464235**	
E. platycephalus	ZMUT.AA11210	Crown	PNG	**PV466646**	**PV464188**	**PV464228**	
E. platycephalus	ZMUT.AA11202	Crown	PNG	**PV466651**	**PV464189**	**PV464244**	
E. platycephalus	ZMUT.AA11206	Crown	PNG	–	**PV464190**	**PV464238**	
E. platycephalus	ZMUT.AA11208	Crown	PNG	**PV466643**	**PV464191**	**PV464239**	
E. platycephalus	ZMUT.AA11177	Crown	PNG	**PV466650**	**PV464192**	**PV464224**	
E. platycephalus	ZMUT.AA11207	Crown	PNG	**PV466652**	**PV464193**	**PV464229**	
E. platycephalus	ZMUT.AA11213	Crown	PNG	**PV466647**	**PV464185**	**PV464236**	
E. platycephalus	ZMUT.AA11203	Crown	PNG	**PV466653**	**PV464194**	**PV464242**	
E. platycephalus	ZMUT.AA11201	Crown	PNG	**PV466649**	**PV464195**	**PV464221**	
E. platycephalus	ZMUT.AA11212	Crown	PNG	**PV466648**	–	**PV464245**	
E. platycephalus	ZMUT.AA11205	Crown	PNG	–	**PV464196**	**PV464223**	
E. platycephalus	ZMUT.AA11200	Crown	PNG	**PV466654**	–	**PV464233**	
E. platycephalus	ZMUT.AA11211	Crown	PNG	**PV466644**	–	**PV464232**	
E. platycephalus	ZMUT.AA11204	Crown	PNG	**PV466655**	–	**PV464230**	
E. platycephalus	ZMUT.AA11216	Tolokiwa	PNG	**PV466641**	–	**PV464247**	
E. platycephalus	ZMUT.AA11217	Tolokiwa	PNG	**PV466639**	**PV464199**	**PV464241**	
E. platycephalus	ZMUT.AA11218	Tolokiwa	PNG	**PV466638**	–	**PV464240**	
E. platycephalus	ZMUT.AA11219	Tolokiwa	PNG	**PV466637**	–	**PV464231**	
E. platycephalus	ZMUT.AA11180	Tolokiwa	PNG	**PV466640**	**PV464197**	**PV464227**	
E. platycephalus	ZMUT.AA11215	Tolokiwa	PNG	–	**PV464198**	**PV464237**	
E. platycephalus	ZMUT.AA11214	Tolokiwa	PNG	**PV466642**	–	**PV464243**	
E. platycephalus	ZMUT.AA11220	Umboi	PNG	**PV466657**	**PV464183**	**PV464246**	
E. platycephalus	ZMUT.AA11221	Umboi	PNG	**PV466656**	**PV464184**	**PV464234**	
Outgroups							**Sequence reference**
Scolopendra cingulata	IZ-131446		Spain	HM453310	HM453220	AF000782	1, 2
Alipes crotalus	IZ-130613		Swaziland	AY288742	AY288720	HM453273	3
Rhysida longipes	CES091395		India	MK273287	MK273411	MK273507	4

(Continued)

Table 1. Continued.

Species	Specimen code	Island	Country	COI	16S	28S	
R. immarginata	CUMZ00436		Thailand	MF167826	MF167759	MF167893	5
Otostigmus astenus	CUMZ00520		Thailand	MF167799	MF167732	MF167866	5
O. spinosus	CUMZ00552		Thailand	MF167784	MF167717	MF167851	5
Sterropristes metallicus	CUMZ00549		Thailand	MF167840	MF167773	MF167907	5
E. tristis	CES08291		India	MH908717	MH908698	MH908713	4
E. tristis	CES08292		India	MH908718	MH908699	MH908714	4
E. tristis	CES08293		India	MH908719	MH908700	–	4
E. tristis	CES0091371		India	MH908730	MH908701	MH908715	4
E. agasthyamalaiensis	CES091099		India	MH908728	MH908696	MH908711	4
E. agasthyamalaiensis	CES091335		India	MH908729	MH908697	MH908712	4
E. agasthyamalaiensis	CES091065		India	MH908726	MH908695	MH908710	4
E. coonooranus	CES091067		India	MH908727	MH908693	–	4
E. coonooranus	CES091063		India	MH908725	MH908692	–	4
E. coonooranus	CES07286		India	JN004031	JN003920	–	4
E. sahyadrensis	CES07279		India	JN004030	JN003919	JN003975	4
E. sahyadrensis	CES08947		India	MH908721	MH908691	MH908708	4
E. sahyadrensis	CES08931		India	MH908720	MH908690	MH908707	4
E. praveeni	CES091391		India	MH908731	MH908689	MH908706	4
E. praveeni	CES091011		India	MH908722	MH908686	MH908703	4
E. praveeni	CES091025		India	MH908724	MH908688	MH908705	4
E. praveeni	CES091012		India	MH908723	MH908687	MH908704	4
E. trigonopodus	AMNH_IZC 00146501		Malawi	HQ402547	HQ402495	–	6
E. rubripes	IZ-130653		Australia	KF676542	KF676475	KF676373	7
E. rubripes	IZ-130652		Australia	AF370836	AY288721	HM453276	8, 3, 1
E. curtipes	WAM115537		Australia	KF676515	KF676474	KF676372	7

Outgroup sequences downloaded from GenBank, with number codes corresponding to the following publications: (1) Murienne et al. (2010), (2) Giribet et al. (1999), (3) Edgecombe and Giribet (2004), (4) Joshi and Edgecombe (2018), (5) Siriwut et al. (2018), (6) Vahtera et al. (2012), (7) Vahtera et al. (2013), and (8) Giribet et al. (2001).

50 independent hits of the shortest tree were found. A strict consensus of the most-parsimonious (MP) trees was produced at the end of the analysis. Nodal supports were estimated with jackknife resampling method (Farris *et al.* 1996) with 1,000 replicates and with a probability of a character removal being 0.36.

For the likelihood analysis, RAxML v. 8 (Stamatakis 2014) via the CIPRES portal (Miller *et al.* 2010) was used. A unique general time-reversible (GTR) model of sequence evolution was applied (RAxML implements only GTR-based models of nucleotide substitutions) with corrections for a discrete gamma distribution (GTR + Γ). Nodal support values were estimated using the rapid bootstrap algorithm with 1,000 replicates together with the GTR-GAMMA model (Stamatakis *et al.* 2008).

Two different species-delimitation methods and 3 different analyses were used to test proposed species boundaries, 1 tree-based and the other distance-based. The first one was multi-rate Poisson tree processes (mPTP) method (Kapli et al. 2017) conducted on the web server (http://mptp.h-its.org) using a phylogeny based on combined- as well as single-locus (COI) datasets. mPTP was used as a model for species delimitation. The second method was Assemble Species by Automatic Partitioning (ASAP) (Puillandre et al. 2021), which builds species partitions from single-locus (COI) alignments. Kimura (K80) was used as the substitution model to compute the distances. ASAP was accessed on the web server https://bioinfo.mnhn.fr/abi/public/asap. In evaluating species, we used the most conservative (ie fewest species) estimate in any of the 3 analyses.

Results

Systematics

Family Scolopendridae Leach (1814)

Subfamily Otostigminae Kraepelin (1903)

***Ethmostigmus* Pocock (1898)**

Type species. *Scolopendra trigonopoda* Leach (1817).

Remarks. A literature survey of previously named *Ethmostigmus* from New Guinea and adjacent islands (eg in North Maluku Province, Indonesia) by Schileyko and Stoev (2016) listed 8 valid species or subspecies: *Ethmostigmus granulosus* Pocock (1898), *Ethmostigmus pygomegas* (Kohlraush 1878), *Ethmostigmus rubripes* (Brandt 1840), including the 2 subspecies *E. r. rubripes* (Brandt 1840) and *Ethmostigmus r. platycephalus* (Newport 1845), *E. telior* (Chamberlin 1939), and *E. venenosus* (Attems 1897). They treated other nominal species from the region as synonyms (eg *E. relictus* Chamberlin 1944) or provisionally valid (*Ethmostigmus rugosus* Haase 1887 and *E. spinosus nannus* Chamberlin 1939). To these, we add 2 new species and treat *E. platycephalus* at the specific rather than subspecific rank.

***Ethmostigmus arboreus* sp. nov.**

(Figs 3 and 4)

http://zoobank.org/urn:lsid:zoobank.org:act:D0394C25-03E3-4D71-848B-C50DC6A67297

Diagnosis. *Ethmostigmus* with arboreal habits; sternal paramedian sulci distinctly impressed along at least half length of sternite from SS4 to 5, consistently strongly defined from SS6 to 7, impressed along at least 75% length of sternite in posterior trunk segments, often as much as 85%; legs relatively long, leg 20 2.78 to 3.39 times length of cephalic plate; 2 pairs of tarsal spurs confined to legs 1 to 3; last tarsal spur usually on leg 19.

Type material. HOLOTYPE: ZMUT.TYPE964 (Figs 3A, D, and G and 4C and E). Papua New Guinea: Madang Prov., Crown Island, 5.132400, 146.968041, 10. –18.iii.2018, coastal/lowland rainforest, V. Weijola leg.

PARATYPES: Specimens ZMUT.TYPE965, ZMUT.TYPE966. Collecting information: same data as for holotype.

Other Material Examined (registration numbers refer to single specimens): ZMUT.AA11181, ZMUT.AA11187, ZMUT.AA11193 to ZMUT.AA11195, all from Tolokiwa; ZMUT.AA11179, ZMUT.AA11182, ZMUT.AA11188 to ZMUT.AA11192, all from Sakar; ZMUT.AA11178, ZMUT.AA11183 to ZMUT.AA11186, all from Umboi.

Etymology. The trivial epithet is a Latin masculine adjective chosen in recognition of the tree-dwelling status of this species.

Description. Length to 165 mm (holotype 130 mm).

Cephalic plate and tergites pale to medium brown; antennae mostly light brown, glabrous articles darker than distal hirsute ones (Fig. 4A); forcipular segment dark orange; sternites yellow-brown to pale orange. Locomotory leg color variation: specimens from Umboi have distinctly blue legs (Fig. 3F), often including the ultimate legs; legs of specimens from Crown light/yellowish brown (Fig. 3A and G); specimens from Tolokiwa and Sakar have darker/olive brown legs.

Most commonly 20 antennal articles, but 17, 18, and 19 observed in 1 or both antennae of a few specimens; basal 4 articles glabrous dorsally (Fig. 3A) and 3 ventrally. Cephalic plate and tergites smooth, punctate. Longitudinal median furrow on anterior fifth of cephalic plate.

Forcipular coxosternal tooth-plates 1.4 to 1.5 times longer than wide, with 3 main teeth, the outermost smaller compared with the inner 2 teeth; a well-defined cusp on the inner tooth (Fig. 3D); base of tooth-plates defined by oblique sutures diverging at 110° (Fig. 3B and C); median suture on coxosternite extending behind base of tooth plates. Second maxillary claw with slender accessory spurs.

T1 overlapping cephalic plate; transverse fold across the anterior margin of T1 shallow or indistinct. Tergites with paramedian sutures along 85% or more of T3, complete from TT4 to 20. Tergites fully marginate starting from TT[6] 7 to 8, with incipient margins as far anteriorly as T5. Paramedian sulci are distinctly impressed from S4, half or more length of sternites from S5 (Fig. 3E), and are nearly complete on posterior half of the trunk (Fig. 3F and G).

Tergite of the ultimate leg-bearing segment 1.5 to 1.8 times wider than long, with parallel or faintly divergent lateral margins, variably rounded posteromedially (Fig. 4B), sometimes with a nearly transverse median extent (Fig. 4A). Sternite of ultimate leg-bearing segment slightly shorter than wide, lateral margins convergent, weakly convex (Fig. 4E to G); posterior margin broadly V-shaped with an angle of 110 to 120°; longitudinal median furrow along half or more length of sternite (Fig. 4E).

Coxopleural process 2 to 3 times longer than the sternite of the ultimate leg-bearing segment (Fig. 4E to G), with 2 apical spines; usually 1 subapical dorsal spine, rarely absent on 1 or both sides or with 2 subapical spines (Fig. 4C); the subapical dorsal spine is usually distinctly separated from the apical spines, but in some specimens, the 3 are close together; 2 (rarely 1 or 3) lateral spines, the posterior of which is variably displaced toward the ventral surface of the coxopleural process; additional dorsal spines rare (1 on one side in a Tolokiwa specimen). Pores dense; non-porose area on process a narrow strip more than a third to half the length to posterior margin of sternite of ultimate leg-bearing segment.

Ultimate legs long; in the holotype, prefemur 9.1 mm, femur 7.0 mm, tibia 4.9 mm, tarsus 1 3.2 mm, tarsus 2 1.7 mm, pretarsus 1.5 mm; tarsus 2 consistently about half the length of tarsus 1. Prefemur with large spines, as follows: VL3, an isolated spine between the VL and VM rows, VM2, M2, DM2, corner spine typically larger than other spines (Fig. 4A and D).

First 2 or 3 pairs of legs with 2 tarsal spurs, 2 spurs on leg 1 only on 1 side of the body in a few specimens, legs (3)4 to 19 with 1 tarsal spur, apart from 2 specimens with last spur on leg 17 or 18; leg 20 only exceptionally with a tarsal spur (ZMUT.AA11191, Sakar). Leg 1 with 1 tibial spur, usually 1 femoral spur, and occasionally a minute prefemoral spur.

Discussion. *Ethmostigmus arboreus* sp. nov. and sympatric *E. platycephalus* are identical with respect to most taxonomic characters used for distinguishing between species of the genus. These include the number of antennal articles (most commonly 20, more rarely 17, 18, or 19), the number of glabrous articles (4 dorsally), dentition of the coxosternal tooth plates (3 teeth, the innermost with a well-defined inner cusp), tergal paramedian sutures (nearly complete on T3, complete from T4), tergite margination (usually incomplete margins on T5 and T6, complete from T7), length and shape of the coxopleural process (2 to 3 times the length of the sternite of the ultimate leg-bearing segment) and its spine distribution (2 apical spines; usually 1 subapical dorsal spine, 2 lateral spines), and spines on the ultimate leg prefemur (VL3, VM2, M2, DM2, and a corner spine of the same size in both species). Most of these character states are also shared by *Ethmostigmus krausi* sp. nov. We regard these characters as diagnostic of a clade that unites these species and have accordingly not used them in species diagnoses.

Two morphological characters consistently distinguish *E. arboreus* from *E. platycephalus*: the depth and length of the sternal paramedian sulci and leg length. Schileyko and Stoev (2016) observed the former character to vary in *E. platycephalus* from being indistinct to being well impressed along two-thirds of the length of the sternites. We identify the same maximal expression of the sulci in *E. platycephalus* (eg ZMUT.AA11180, from Tolokiwa), but it is possible to separate specimens of the 2 species by the sulci being longer on the same trunk segment in *E. arboreus* than in *E. platycephalus* (eg Figs 3E versus 5B and 3F versus 5C). Sulci are consistently strongly impressed and long from sternites 6 or 7 in *E. arboreus*. Ordination analyses detailed below reveal longer legs in *E. arboreus* than in *E. platycephalus*; in *E. arboreus*, the length of leg 20 relative to the cephalic shield ranges from 2.78 to 3.39 (mean

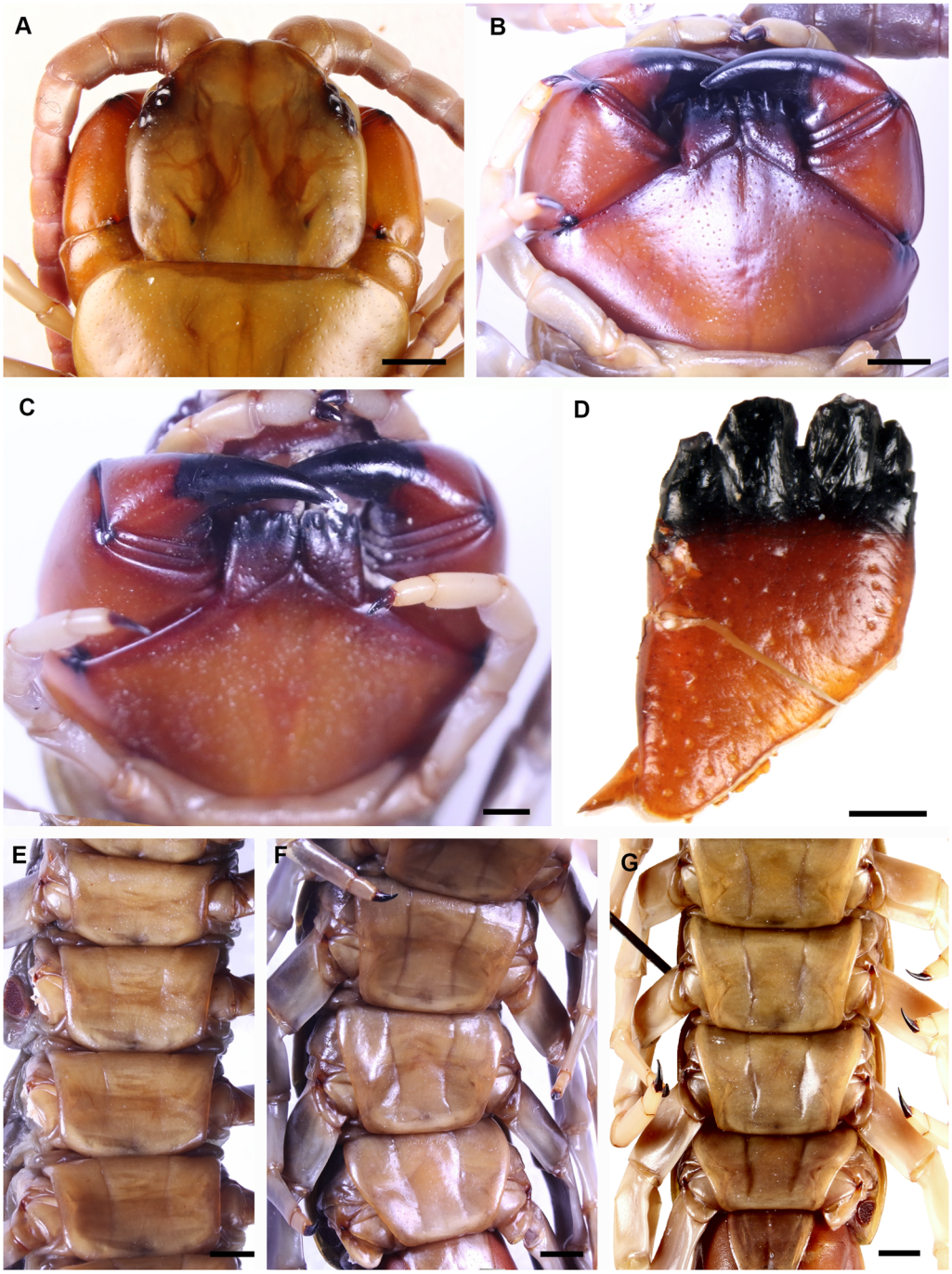

Fig. 3. *Ethmostigmus arboreus* sp. nov. A, D, G) holotype, ZMUT.TYPE964 (Crown); B, E, F) ZMUT.AA11181 (Tolokiwa); C) ZMUT.AA11188 (Sakar). A) dorsal view of cephalic plate and forcipular segment; B, C) ventral view of forcipular segment; D) tooth-plate; E, F) ventral views of SS4 to 7 and 17 to 20, respectively; G) ventral view of SS17 to 21. Scale bars 2 mm except C, 1 mm, D, 0.5 mm.

3.05), whereas the corresponding range for *E. platycephalus* in our sample is 2.33 to 3.12 (mean 2.62). The distribution of tarsal spurs provides 2 additional subtle differences: *E. arboreus* has not been observed to have 2 tarsal spurs posterior to leg 3, whereas sympatric *E. platycephalus* frequently has 2 spurs on leg 4 and exceptionally has 2 spurs on leg 5, and the last tarsal spur is overwhelmingly on leg 19 in *E. arboreus* versus equal frequencies on leg 19 or 20 in *E. platycephalus*.

Among available species names, *Ethmostigmus browni* (Butler 1877) is potentially available for the species here treated as *E. arboreus*. The type of *Heterostoma browni* (BMNH #200567 Chilo. 188-35), from Duke of York Island between New Britain and New Ireland, has been identified as a junior subjective synonym of *E. platycephalus* since Pocock (1899). It resembles *E. arboreus* in its nearly complete sternal sulci in posterior trunk segments, sulci >70% the length of sternite 5, as well as meristic characters that both share with *E. platycephalus*. The antennal article count (18/18) of the *E. browni* holotype is matched by Tolokiwa specimen ZMUT.AA1181; while 20 articles on at least 1 antenna is usual for *E. arboreus*, this character does not

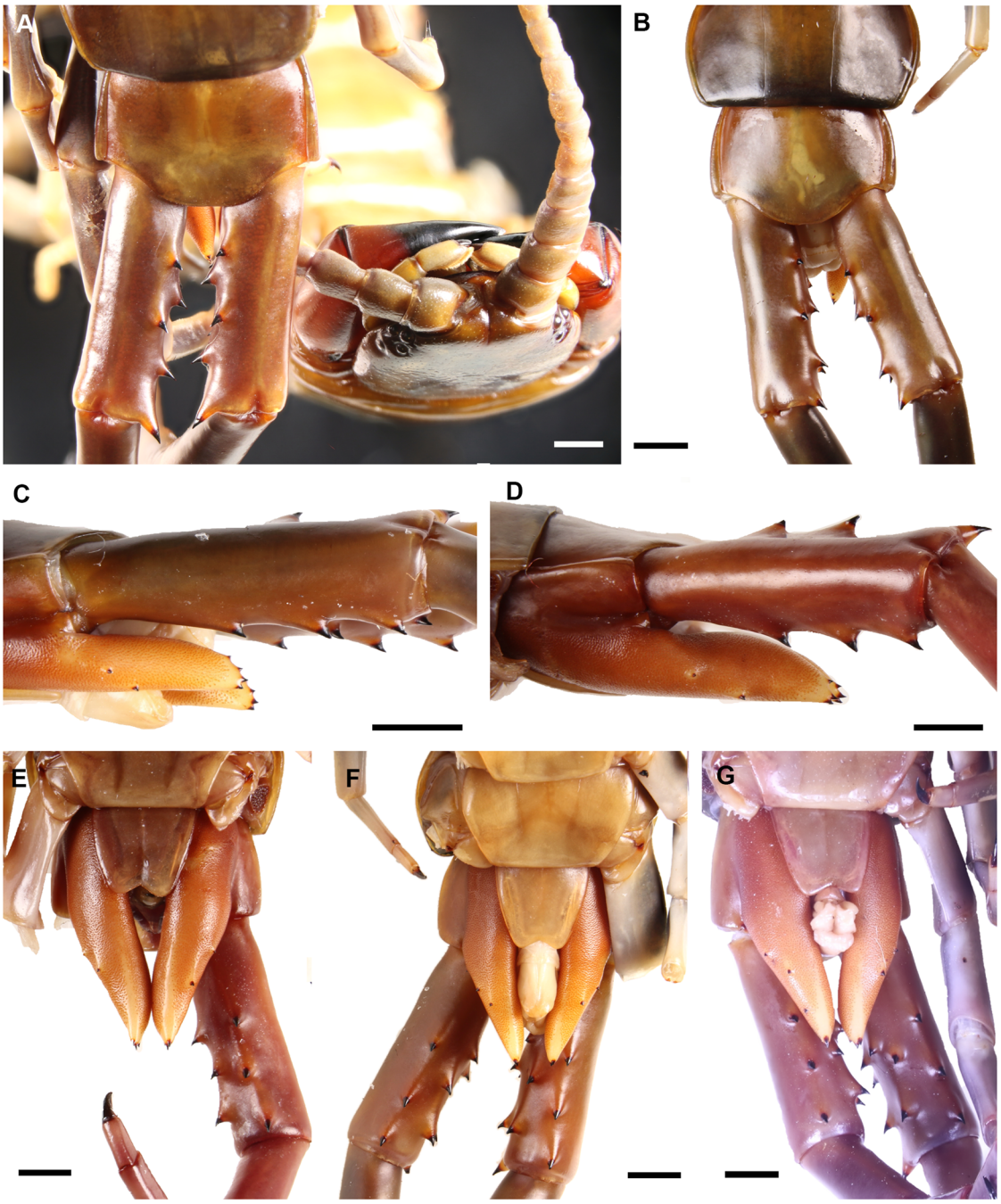

Fig. 4. *Ethmostigmus arboreus* sp. nov. A) ZMUT.AA11181 (Tolokiwa); B, D, F) ZMUT.AA11184 (Umboi); C, E) holotype, ZMUT.TYPE964 (Crown); G) ZMUT.AA11188 (Sakar). A) dorsal view of ultimate leg-bearing segment and anterior view of head; B) dorsal view of ultimate leg-bearing segment; C, D) lateral view of coxopleuron and prefemur of ultimate leg; E to G) ventral views of S20 and ultimate leg-bearing segment. Scale bars 2 mm.

separate these species. *Ethmostigmus browni* also has relatively elongate legs (leg 20 is 3.16 times the length of the cephalic plate). The coxopleural process of the *E. browni* type has 2 apical and 2 subapical dorsal spines, the latter uncommon (but present) in *E. arboreus*. Paired tarsal spurs are confined to legs 1 and 2, as is common in *E. arboreus*. Our molecular and ecological data from records in the Bismarck volcanic arc, combined with the morphological arguments made above, suggest that *E. browni* may warrant revalidation as distinct from *E. platycephalus*, as long sternal sulci, long legs, and paired tarsal spurs confined to anterior leg pairs are of taxonomic value in *Ethmostigmus* in this region. Without molecular data from the type locality of *E. browni*, ca. 500 km east of the most easterly record of *E. arboreus*, and no observations on whether *E. browni* is arboreal, we have treated *E. arboreus* as a new species rather than applying a name that has not been in use for 125 years. Using the morphometric criteria applied to legs 6 and 20 of the Bismarck volcanic arc samples, the holotype of *E. browni* falls outside the range of variation of *E. arboreus* with respect to some proportions, notably the relative length of leg 20 tarsus 1 and femur (0.557 in *E. browni* versus 0.603 to 0.708 in *E. arboreus*).

Among other named species, *Ethmostigmus wainanus* Chamberlin (1920), from the Solomon Islands, shares elongate, deeply impressed sternal paramedian sulci with *E. arboreus* (and *E. browni*). Photographs of the types at the Museum of Comparative Zoology were kindly provided by Dr L. Benavides

for comparison. Tarsal spurs provide the most obvious distinction, Chamberlin's (1920) description of *E. wainanus* indicating no legs with paired tarsal spurs, and the lack of a tarsal spur on leg 19 (rare in *E. arboreus*).

Ethmostigmus platycephalus **(Newport 1845)**

(Fig. 5)

Material Examined (registration numbers refer to single specimens): ZMUT.AA11197, ZMUT.AA11198 (both from KarKar); ZMUT.AA11177, ZMUT.AA11199 to AA11213 (all from Crown), ZMUT.AA11180, ZMUT.AA11214 to ZMUT.AA11219 (all from Tolokiwa); ZMUT.AA11220, ZMUT.AA11221 (both from Umboi).

Discussion. Newport's holotype of *Heterostoma platycephala* is unknown, and its type locality is no more precise than the islands in the Pacific ("In Insuls Oceani Pacifici"). A specimen in the NHMUK collection thought to be the type by Joshi and Edgecombe (2018, Fig. 3) has no definitive type status. Despite these serious ambiguities, the concept of *E. platycephalus* has

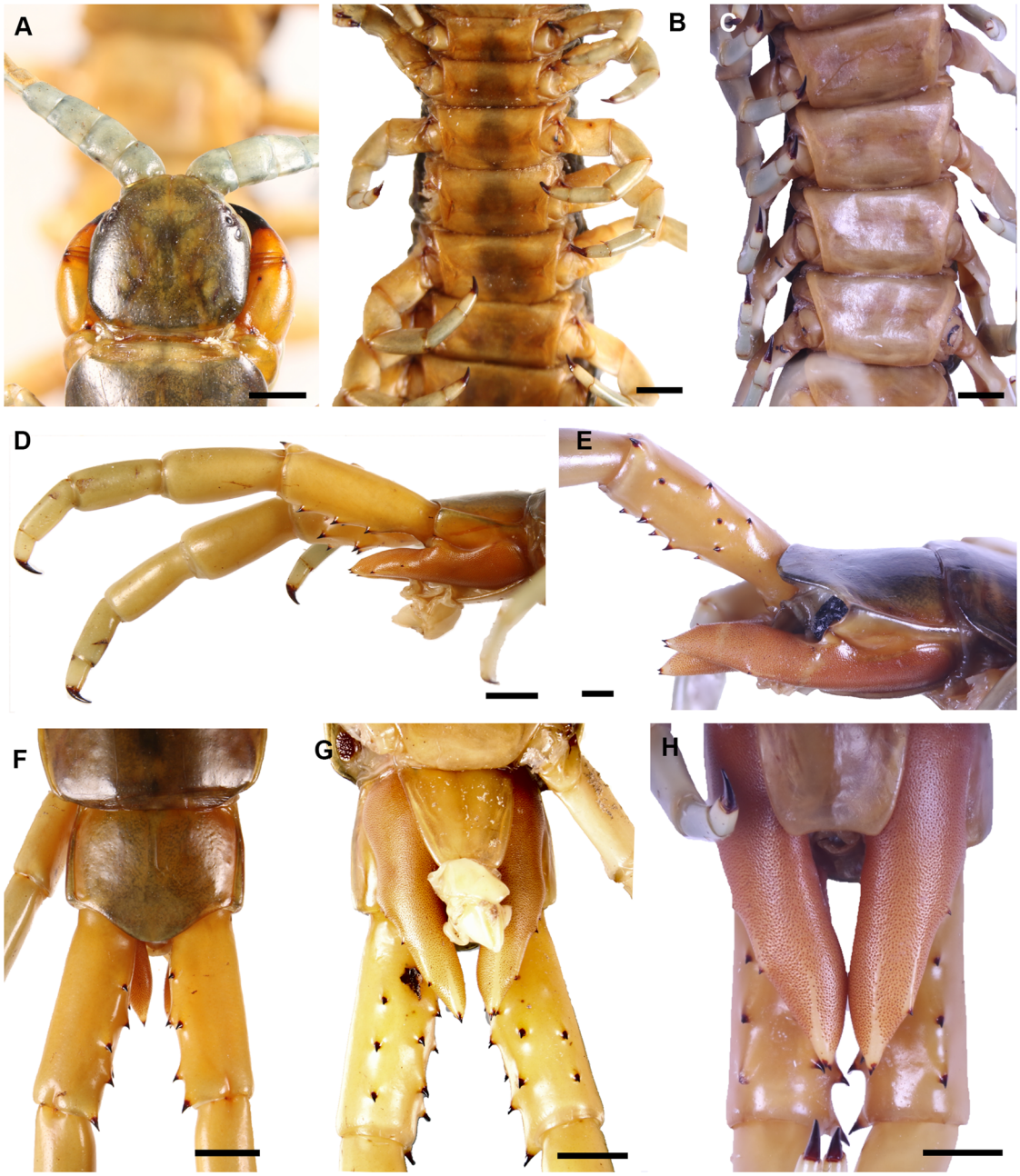

Fig. 5. *Ethmostigmus platycephalus* (Newport 18454). A, D, F, G) ZMUT.AA11206 specimen (Crown); B, E) ZMUT.AA11207 specimen (Crown); C) ZMUT.AA11219 specimen (Tolokiwa); H) ZMUT.AA11217 specimen (Tolokiwa). A) Dorsal view of cephalic plate, antennae, and forcipular segment; B) Ventral view of SS1 to 8; C) ventral view of SS16 to 20; D) Lateral view of ultimate leg-bearing segment; E) lateral view of ultimate leg-bearing segment and ultimate leg prefemur; F) dorsal view of T20, ultimate leg-bearing segment and ultimate leg prefemora; G, H) ventral views of ultimate leg-bearing segment and ultimate leg prefemora. Scale bars 2 mm.

a coherent evolution of usage over the past century, the name and morphological concept here corresponding to *E. platycephalus platycephalus* sensu Attems (1930) and *E. rubripes platycephalus* of Schileyko and Stagl (2004). Without molecular data for almost all populations that correspond to this morphology-based taxonomic concept, we apply the name i*E. platycephalus* to the ground-dwelling species in our samples that matches the scope of that species following the most recent taxonomic treatment of New Guinea material (Schileyko and Stoev 2016). Because of its widespread geographic range and likelihood of variability beyond that in our island populations, we have not formally rediagnosed *E. platycephalus*. Its distinguishing characters relative to the otherwise most similar, closely related, and sympatric *E. arboreus* are cited in the "Discussion" section under the latter species.

***Ethmostigmus krausi* sp. nov.**

(Figs 6 and 7)

https://zoobank.org/urn:lsid:zoobank.org:act:4F394ABFB9B1-4CC7-A5A6-1E5075D53909

Diagnosis. *Ethmostigmus* with conspicuous punctae on cephalic plate and T1; lateral parts of trunk tergites from T3 with irregular longitudinal rugose ridges bearing coarse granules; fine granules sparsely scattered amidst the coarse granules.

Type material. HOLOTYPE: Specimen ZMUT.TYPE967 (Figs 6A and 7B, C, and E). Papua New Guinea: Morobe Prov., Sakar Island, –5.411894, 148.114386, 4.4. –12.iv.2018, coastal/lowland rainforest, V. Weijola leg.

PARATYPES: Specimens ZMUT.TYPE968 to ZMUT.TYPE973. Papua New Guinea: Morobe Prov., Umboi Island, –5.712854, 148.067349, 30.iii. –3.iv./13. –19.iv.2018, coastal/lowland rainforest, V. Weijola leg.

Etymology. The specific name is a patronym in honor of Dr Fred Kraus (University of Michigan) and his extensive contributions to our understanding of the herpetofauna of Papua New Guinea.

Description. Length to 110 mm (holotype).
Cephalic plate and T1 are dark olive green in the holotype (Sakar: Fig. 6A) and some Umboi specimens (ZMUT.TYPE968), with the following tergites showing mixed brown and green pigmentation; in holotype, antennae are mostly pale orange, glabrous articles olive green, and legs olive green from prefemur to tibia, with yellow tarsi; Umboi specimens are variably with dark purplish brown cephalic plate and tergites (Fig. 6E and F) and pale orange legs.

Twenty antennal articles; the basal 4 articles are glabrous dorsally (Fig. 6A) and 3 ventrally (Fig. 6B). Cephalic plate and T1/T2 conspicuously punctate (Fig. 6A). Longitudinal median furrow on anterior 15% of cephalic plate.

Forcipular coxosternal tooth-plates 1.4 to 1.6 times longer than wide (Fig. 6B and D), with 3 main teeth, the outermost smaller compared with the inner 2 teeth; a well-defined cusp on the inner tooth; base of tooth-plates defined by oblique sutures diverging at 110°; median suture on coxosternite extending behind base of tooth plates. Second maxillary claw with slender accessory spurs.

T1 with slight to distinct overlap of cephalic plate; transverse fold across anterior margin of T1 shallow to moderately impressed (Fig. 6A). Tergites with paramedian sutures nearly complete on T3 and complete from TT4 to 20. Tergites fully marginate, starting from TT[6] 7 to 8, with incipient margins as far anteriorly as T5. Irregular longitudinal ridges on tergites as far anteriorly as T3, more pronounced from TT6 to 7 (Fig. 6C, F, and G); coarsest granules concentrated on ridges, but coarse granules scattered on the median, non-rugose part of tergites as well. Paramedian sulci are well impressed along the length of the trunk, 50–ca 75% the length of the sternites (Fig. 7A to C).

Tergite of the ultimate leg-bearing segment is about 2.4 times wider than long, with parallel lateral margins, rounded posteromedially (Fig. 7F). The sternite of the ultimate leg-bearing segment is slightly shorter than wide, posterior margins concave with an angle of 140 to 150°; longitudinal median furrow is present (Fig. 7G).

Coxopleural process 2.6 to 3.1 times the length of sternite of the ultimate leg-bearing segment (Fig. 7G and H), with 2 apical spines (1 on 1 side in 1 specimen); 1 subapical dorsal spine variably present or absent; 2 lateral spines (1 on 1 side in 1 specimen), the posterior of which is variably displaced toward the ventral surface of the coxopleural process. Pores dense; non-porose area on process a narrow strip 24% to 29% the length to the posterior margin of the sternite of the ultimate leg-bearing segment.

Ultimate legs long, in holotype, prefemur 11.1 mm, femur 7.6 mm, tibia 5.8 mm, tarsus 1 3.7 mm, and tarsus 2 2.1 mm; tarsus 2 consistently slightly more than half length of tarsus 1; pretarsus about equal in length to tarsus 2. Prefemur with large spines, as follows: VL3, VM2, M2, and DM2 (Fig. 7E to H). Corner spine larger than other spines (Fig. 7E and F).

First 1 or 2 pairs of legs with 2 tarsal spurs, legs (2)3 to 19 with 1 tarsal spur apart from 1 specimen with tarsal spur on leg 20 (ZMUT.TYPE970, from Umboi). Leg 1 with 1 tibial spur, usually 1 femoral spur, and sometimes a minute prefemoral spur.

Discussion. Another granulate species, *E. granulosus* Pocock (1899), from New Britain, is not conspecific with the Umboi and Sakar specimens assigned to *E. krausi*. *Ethmostigmus krausi* has coarse granulation, especially on the posterior half of its trunk, versus much finer granulation and less pronounced rugose ridges in *E. granulosus*, based on a study of the type, BMNH(E) #200065 Chilo.1898.16.6.6. They are further distinguished by *E. krausi* having 3 VL spines (Fig. 7G and H) on the ultimate leg prefemur (versus 2 in *E. granulosus*), 2 versus 1 lateral spine on each coxopleural process, and the "very obsoletely bisulcate" sternites described by Pocock (1899) for *E. granulosus* that involve a pair of notches along no more than the anterior 10% of the sternites, versus elongate sulci in *E. krausi*.

Ethmostigmus rugosus (Haase 1887) was based on a type from Halmahera in the Moluccas, Indonesia. Its specific name refers to coarse longitudinal wrinkles ("runzlig" fide Haase 1887) on the tergites. Examination of the holotype, RMNH.CHIL.99 (Naturalis Biodiversity Center, Leiden), by C.A.M-M. indicates that these wrinkles are present on tergites 3 to 14 but become less distinct from ca tergite 13, and the coarse granulation of *E. krausi* is not present in *E. rugosus*. The long, tapering forcipular tooth-plates in the holotype of *E. rugosus* (Haase 1887, fig. 96a) also distinguish it from *E. krausi*, in which the

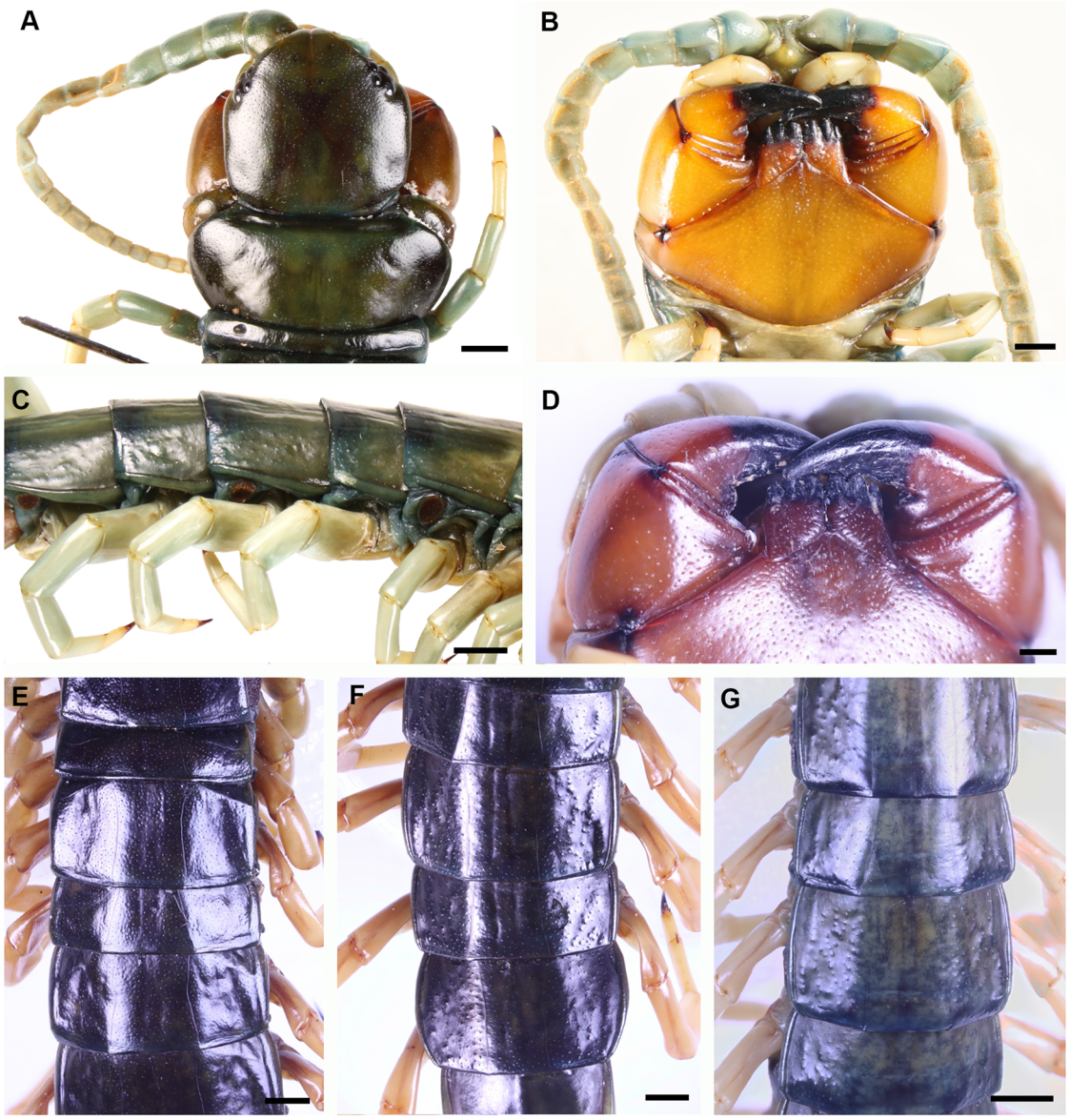

Fig. 6. *Ethmostigmus krausi* sp. nov. A) Holotype, ZMUT.TYPE967 (Sakar); B, C) specimen ZMUT.TYPE968 (Umboi); D to F) ZMUT.TYPE972 (Umboi); G) ZMUT.TYPE973 (Umboi). A) dorsal view of cephalic plate, antenna, and forcipular segment. B) Ventral view of forcipular segment and antennae. C) Lateral view of segments 16 to 20. D) ventral view of forcipular segment. E, F) Dorsal view of TT3 to 8 and 17 to 21, respectively. G) Dorsal view of TT15 to 19. Scale bars 2 mm except B, D, 1 mm.

tooth plates are distinctly wider. Another congener with types from Halmahera, *E. venenosus* (Attems 1897), is readily distinguished from all 3 species considered herein by the presence of 5 to 7 dorsal spines on the coxopleural process (versus 1 subapical dorsal spine).

Morphometric Analyses

Tukey's multiple comparisons of means showed significant differences between species in terms of the size-adjusted lengths of several limb articles (Table 2). The largest interspecific differences were found between the arboreal *E. arboreus* and the terrestrial *E. platycephalus*, where total limb length and the length of all articles except for the LP6 tibia of *E. arboreus* were significantly longer compared to *E. platycephalus*. The largest differences are found in the prefemora, which were on average 21.1% (leg 20) and 19.4% (leg 6%) longer in *E. arboreus*. Total limb length differences were 12.3% (LP6) and 15.0% (LP20).

Ethmostigmus arboreus also had longer total limb lengths by 7.8% (LP6) and 7.0% (LP20), a longer prefemur by 17.9% (LP6) and 17.5% (LP20), and longer LP20 femur (by 6.5%) than *E. krausi*.

The largest significant differences between *E. krausi* and *E. platycephalus* were found in the lengths of the tarsi, with differences of 8.2% (tarsus 2, LP6), 13.0% (tarsus 1, LP20), and 11.1% (tarsus 2, LP 20) and were always longer in *E. krausi*. Only in LP20 was the total limb length significantly longer (by 8.1%) in *E. krausi*.

The LDA clearly differentiated all 3 species in morphological space (Fig. 8). The prior probabilities of each group were 0.39, 0.18, and 0.43 for *E. arboreus*, *E. krausi*, and *E. platycephalus*, respectively. The coefficients of linear discriminants (on LD1

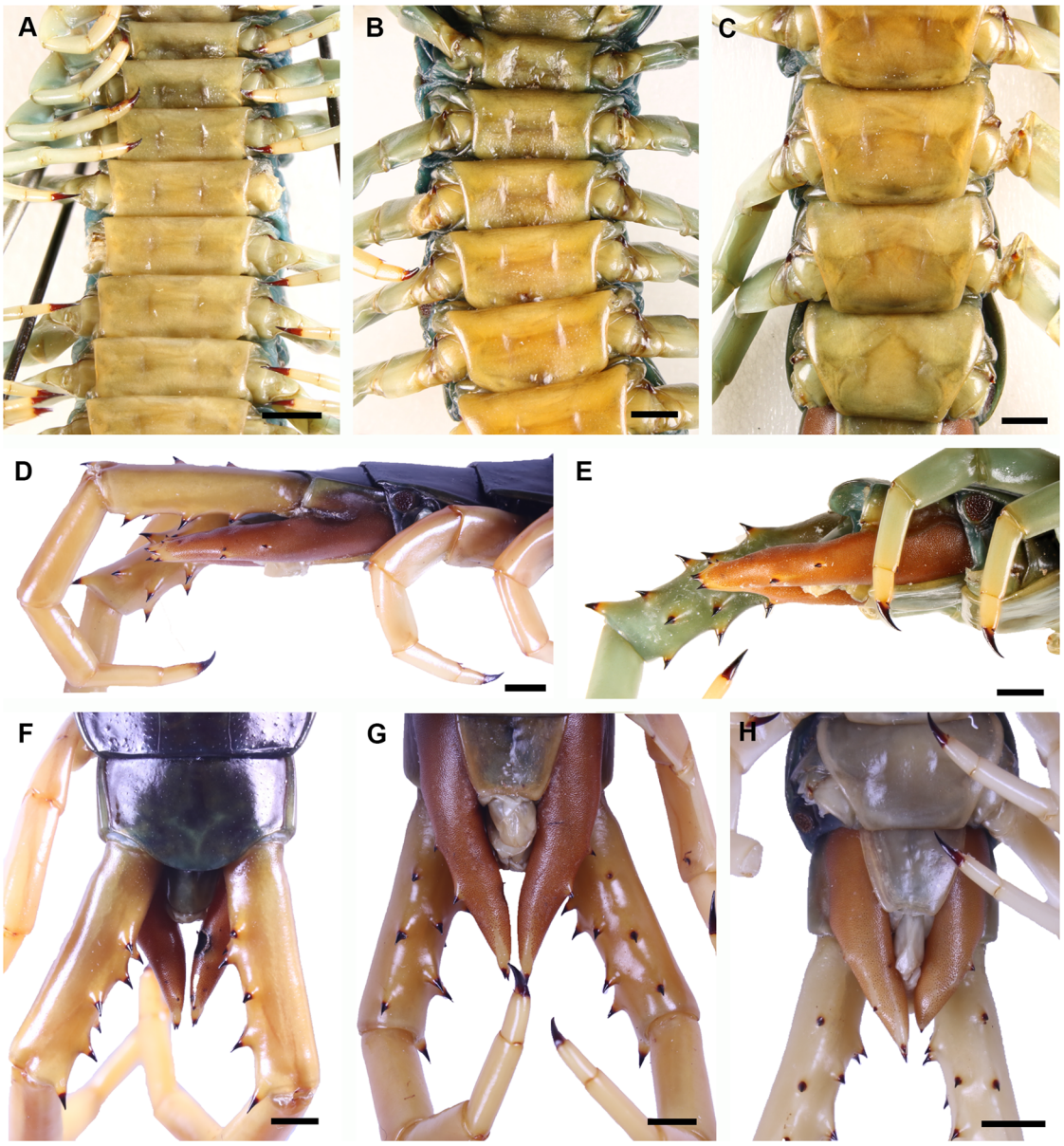

Fig. 7. *Ethmostigmus krausi* sp. nov. A) ZMUT.TYPE968 (Umboi); B, C, E) holotype, ZMUT.TYPE967 (Sakar); D, F, G) ZMUT.TYPE972 (Umboi); H) ZMUT.TYPE973 (Umboi). A to C) Ventral views of SS1 to 9, 1 to 7, and 17 to 20, respectively; D) lateral view of segments 19 to 21 and ultimate legs; E) lateral view of ultimate leg-bearing segment and ultimate leg prefemur; F, G) dorsal and ventral views of ultimate leg-bearing segment; H) ventral view of ultimate leg-bearing segment and ultimate leg prefemora. Scale bars 2 mm.

and LD2) for each morphometric article are shown in Table 3. These revealed that the tibia and femur on LP6 contributed most significantly to the group differences on LDA1, together with the femur and tibia on LP20. The prefemur on LP20 contributed mostly to the differences between species on LDA2. In general, the differences between species were driven more strongly by articles on LP20. Table 3 also includes the singular value decompositions, which give the ratio of the between- and within-group standard deviations on the linear discriminant variables.

Molecular Phylogenetic Analysis

The 2 analyses (likelihood and parsimony) produced congruent phylogenies (Figs 9 and 10). The final ML optimization likelihood was −12053.991575. Parsimony analysis resulted in 5,739 MP trees of length 2,474 steps. In both trees (Figs 9 and 10), specimens belonging to *E. arboreus* form a monophyletic group with strong nodal support (jackknife support [JF from herein] = 98, bootstrap support [BS from herein] = 100). The sister group (JF = 100, BS = 99) to *E. arboreus* is composed of the specimens belonging to *E. platycephalus*. The latter are divided into 2 groups, the first 1 including 2 samples from KarKar (JF = 99, BS = 100) and the second with the remaining samples from Crown, Tolokiwa, and Umboi (JF = 99, BS = 100). The third Papua New Guinean clade includes 6 specimens belonging to *E. krausi* from Umboi and Sakar islands (JF = 100, BS = 100) and is resolved as a sister group (JF = 91, BS = 97) to *E. arboreus* + *E. platycephalus*.

The deeper nodes in the parsimony and likelihood analyses differ slightly with regard to poorly supported nodes.

Table 2. Tukey's multiple test results for all species comparisons and articles

Comparison	Article	p_value	Estimate	% diff. (normalized)	Longer in
E. platycephalus—E. arboreus	LP6 prefemur	**0.001**	−0.494	19.398	*E. arboreus*
E. platycephalus—E. arboreus	LP6 femur	**0.001**	−0.293	12.844	*E. arboreus*
E. platycephalus—E. arboreus	LP6 tibia	0.111	−0.129	6.735	*E. arboreus*
E. platycephalus—E. arboreus	LP6 tarsus1	**0.001**	−0.262	13.648	*E. arboreus*
E. platycephalus—E. arboreus	LP6 tarsus2	**0.006**	−0.105	3.740	*E. arboreus*
E. platycephalus—E. arboreus	LP6 total	**0.001**	−1.283	12.318	*E. arboreus*
E. platycephalus—E. arboreus	LP20 prefemur	**0.001**	−1.054	21.065	*E. arboreus*
E. platycephalus—E. arboreus	LP20 femur	**0.001**	−0.673	13.777	*E. arboreus*
E. platycephalus—E. arboreus	LP20 tibia	**0.001**	−0.596	13.631	*E. arboreus*
E. platycephalus—E. arboreus	LP20 tarsus1	**0.001**	−0.519	14.904	*E. arboreus*
E. platycephalus—E. arboreus	LP20 tarsus2	**0.001**	−0.162	2.612	*E. arboreus*
E. platycephalus—E. arboreus	LP20 total	**0.001**	−3.012	15.023	*E. arboreus*
E. krausi—E. arboreus	LP6 prefemur	**0.001**	−0.482	17.871	*E. arboreus*
E. krausi—E. arboreus	LP6 femur	0.066	−0.187	8.100	*E. arboreus*
E. krausi—E. arboreus	LP6 tibia	0.778	−0.049	3.146	*E. arboreus*
E. krausi—E. arboreus	LP6 tarsus1	0.137	−0.134	6.641	*E. arboreus*
E. krausi—E. arboreus	LP6 tarsus2	0.998	0.002	4.420	*E. arboreus*
E. krausi—E. arboreus	LP6 total	**0.009**	−0.85	7.792	*E. arboreus*
E. krausi—E. arboreus	LP20 prefemur	**0.001**	−0.897	17.498	*E. arboreus*
E. krausi—E. arboreus	LP20 femur	**0.03**	−0.345	6.522	*E. arboreus*
E. krausi—E. arboreus	LP20 tibia	0.075	−0.238	4.549	*E. arboreus*
E. krausi—E. arboreus	LP20 tarsus1	0.233	−0.14	1.959	*E. krausi*
E. krausi—E. arboreus	LP20 tarsus2	0.533	−0.031	8.491	*E. krausi*
E. krausi—E. arboreus	LP20 total	**0.002**	−1.595	6.994	*E. arboreus*
E. platycephalus—E. krausi	LP6 prefemur	0.988	−0.012	1.540	*E. krausi*
E. platycephalus—E. krausi	LP6 femur	0.377	−0.106	4.756	*E. krausi*
E. platycephalus—E. krausi	LP6 tibia	0.491	−0.08	3.591	*E. krausi*
E. platycephalus—E. krausi	LP6 tarsus1	0.146	−0.128	7.023	*E. krausi*
E. platycephalus—E. krausi	LP6 tarsus2	**0.012**	−0.107	8.157	*E. krausi*
E. platycephalus—E. krausi	LP6 total	0.249	−0.433	4.536	*E. krausi*
E. platycephalus—E. krausi	LP20 prefemur	0.403	−0.157	3.600	*E. krausi*
E. platycephalus—E. krausi	LP20 femur	**0.03**	−0.328	7.272	*E. krausi*
E. platycephalus—E. krausi	LP20 tibia	**0.002**	−0.358	9.096	*E. krausi*
E. platycephalus—E. krausi	LP20 tarsus1	**0.001**	−0.379	12.954	*E. krausi*
E. platycephalus—E. krausi	LP20 tarsus2	**0.001**	−0.193	11.097	*E. krausi*
E. platycephalus—E. krausi	LP20 total	**0.003**	−1.417	8.049	*E. krausi*

Significant *P*-values (<0.05) are highlighted in bold. The estimate represents the mean difference in mm between the group means for a specific pairwise comparison.

Parsimony analysis resolves 2 *Ethmostigmus* species from Australia together with an African species, *E. trigonopodus* (JF = 56), as a sister group (JF = 71) to the "Papuan clade," whereas likelihood analysis resolves Australian specimens (BS = 65) as a sister group (BS = 82) to the "Papuan clade," leaving the African *E. trigonopodus* as a sister (BS = 55) to all of them. Deeper in the tree, a clade of 5 *Ethmostigmus* species from the Eastern and Western Ghats of India (JF = 95, BS = 96) is resolved as a sister group (JF = 77, BS = 74) to all other congeners.

Species Delimitation and Taxonomy

Our molecular phylogenetic analyses recover the 3 species from islands of the Bismarck volcanic arc (*E. platycephalus*, *E. arboreus*, and *E. krausi*) as a strongly supported monophyletic group. While there is a distinct possibility that a larger sampling from New Guinea, New Britain, and perhaps even the Solomon Islands, would add further species to this clade, this would not affect the common ancestry and close phylogenetic affinity of the 3 species discussed here. As noted above, the 3 species share a set of conserved morphological characters, including typically 20 antennal articles, of which 4 are glabrous dorsally, paramedian sutures complete from tergite 4, a long coxopleural process with 2 apical spines, 1 subapical dorsal spine, and 2 lateral spines, and ultimate leg prefemoral spines including VL3, VM2, M2, DM2, and a corner spine.

In the species delimitation analyses, the tree with the highest ASAP score, together with passing the set significance threshold, was chosen as preferred, whereas mPTP provided only 1 result. Results from both delimitation methods were in congruence with the new species described here (see Figs 8 and 9). The most conservative results obtained from both mPTP and ASAP analyses showed *E. krausi*, *E. arboreus*, and *E. platycephalus* as distinct species. However, the specimens from Karkar were also suggested to belong to a separate species in the combined mPTP and ASAP analyses. Similarly, the 2 *E. arboreus* specimens from Crown Island were shown as a separate species in mPTP analysis based on COI only and in the ASAP analysis. As noted above, we recognize species boundaries as the fewest recovered in any of the 3 delimitation analyses and by morphological diagnosability.

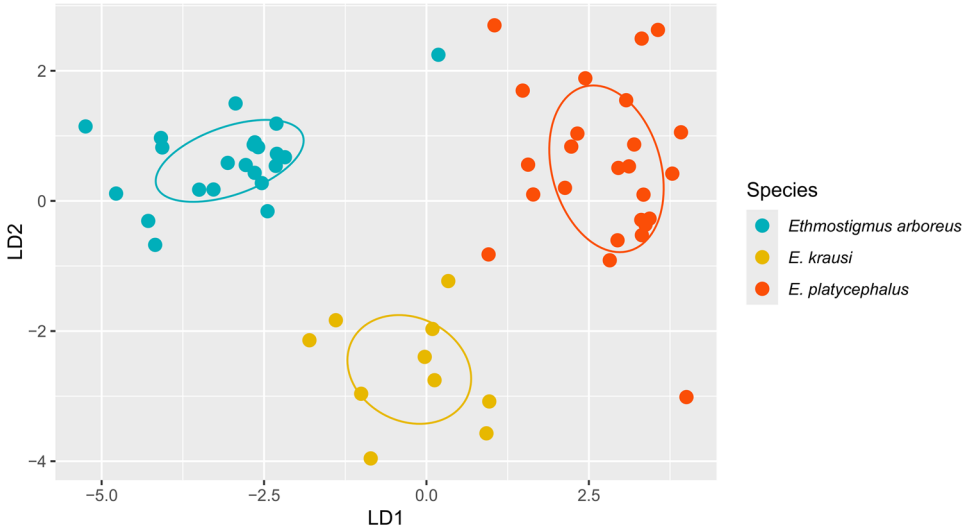

Fig. 8. Linear Discriminant Analysis (LDA) performed on the log normalized morphometric data of the 3 species (*E. arboreus* = blue, *E. krausi* = yellow, *E. platycephalus* = red). The 2 axes represent the first 2 linear discriminants (LD1 and LD2), which are the linear combinations of the original features that best separate the different species. Each point corresponds to an observation, colored according to its class label. The plot shows a distinct clustering of observations based on the species, indicating that LDA effectively separates the differences in the morphological characteristics. LD1 explains 83.2% of the between-species variability, while LD2 explains 16.8% of the variability, suggesting that these 2 components capture a significant portion of the differences.

Table 3. The coefficients of linear discriminants provide insights into how the original features (articles) contribute to the linear discriminants, which are the new axes that maximize the separation between the species

Leg article	LDA 1	LDA 2
LP6 prefemur	14.77598	13.123997
LP6 femur	46.00419	6.086669
LP6 tibia	52.79578	−42.820031
LP6 tarsus 1	19.56369	−9.072617
LP6 tarsus 2	−30.625095	10.645016
LP6 total length	−81.62398	47.745855
LP20 prefemur	252.42826	263.427914
LP20 femur	308.33044	250.219403
LP20 tibia	261.18178	225.877751
LP20 tarsus 1	149.24094	135.004267
LP20 tarsus 2	80.62093	44.641774
LP20 total	−1125.21303	−951.380282
SVD	12.08	4.75
Proportion of trace	0.8315	0.1685

The singular value decompositions (SVD) are indicative of the strength and importance of each discriminant in explaining the between-species variance. The proportion of trace shows the proportion of the total variance explained by each linear discriminant (LD) in the LDA model.

Species delimitation in *Ethmostigmus* has mostly been based on morphology alone and conducted in a framework in which species are conceptualized as geographically widespread and polymorphic. Traditional taxonomic practice would assign *E. platycephalus* in our samples and likely also *E. arboreus* to *E. rubripes platycephalus* (Newport 1845), as in the recent taxonomic description of material from New Guinea and adjacent islands (Schileyko and Stoev 2016). Therein, *E. rubripes platycephalus* is conceived as distributed across Tahiti, the Solomon Islands, New Guinea, the Bismarck Archipelago, eastern Indonesia, the Philippines, Spratly Island, possibly Australia, Sri Lanka, Laos, Vietnam, Cambodia, and China. A specimen from Umboi was assigned to *E. rubripes platycephalus* by Schileyko and Stagl (2004). Herein, we recognize *E. platycephalus* as a species separate from *E. rubripes*. Australian material of *E. rubripes* (*E. rubripes rubripes* sensu Schileyko and Stagl 2004) is not resolved in our phylogenetic analyses as most closely related to New Guinea material that corresponds morphologically and geographically to *E. platycephalus*, and we find it to be sister to *Ethmostigmus curtipes*. Our phylogenetic results suggest that species are more morphologically and genetically discrete than has been captured in taxonomy predicated on subspecies intergrading morphologically across vast geographic ranges.

Drawing on multi-locus sequence data as well as morphology in an integrative taxonomic framework, species of *Ethmostigmus* in the Western Ghats, India, were found to consist of clades with narrower, almost wholly allopatric geographic distributions and subtle, but diagnostic, morphological characters (Joshi and Edgecombe 2018). Our data from the Bismarck Archipelago are consistent with this species delimitation concept, finding that 3 sympatric species share a suite of conserved phenotypic characters, but are readily identified based on molecular phylogeny, in which they form clearly separated clades. We have elected to name 2 of them as new species, having morphological and/or ecological traits that allow for their diagnosis from other named species. Between-group mean distances of COI/16S sequences are 15.3%/10.3%, respectively, for *E. krausi* and *E. arboreus*, 12.5%/12.9% for *E. krausi* and *E. platycephalus*, and 10%/9.1% for *E. arboreusi* and *E. platycephalus*. These distances approximate those between the Western Ghats species, which are 17.3%/9.4%, respectively, for *Ethmostigmus coonooranus* and *Ethmostigmus praveeni*, 15%/10% for *E. coonooranus* and *Ethmostigmus sahyadrensis*, and 14.2%/9.4% for *E. praveeni* and *E. sahyadrensis*. Within-group distances for COI/16S sequences are 4%/1% for *E. arboreus* and 2%/1% for *E. platycephalus* (*E. krausi* sequences were identical).

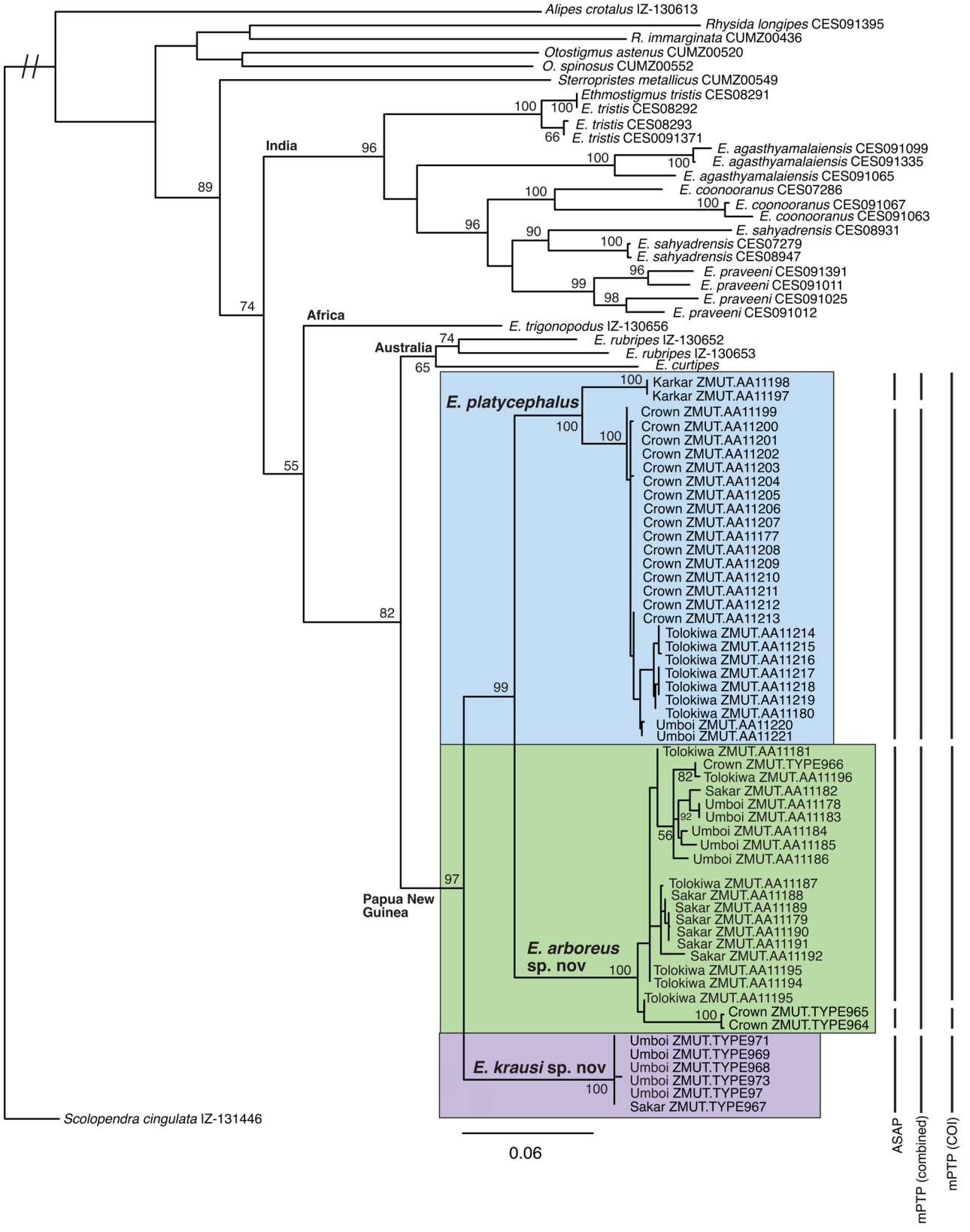

Fig. 9. Likelihood-based phylogeny of *Ethmostigmus* species and outgroups based on COI, 16S, and 28S sequence data. Numbers at nodes are bootstrap support. Bars at the right margin show the species delimitations by ASAP and mPTP.

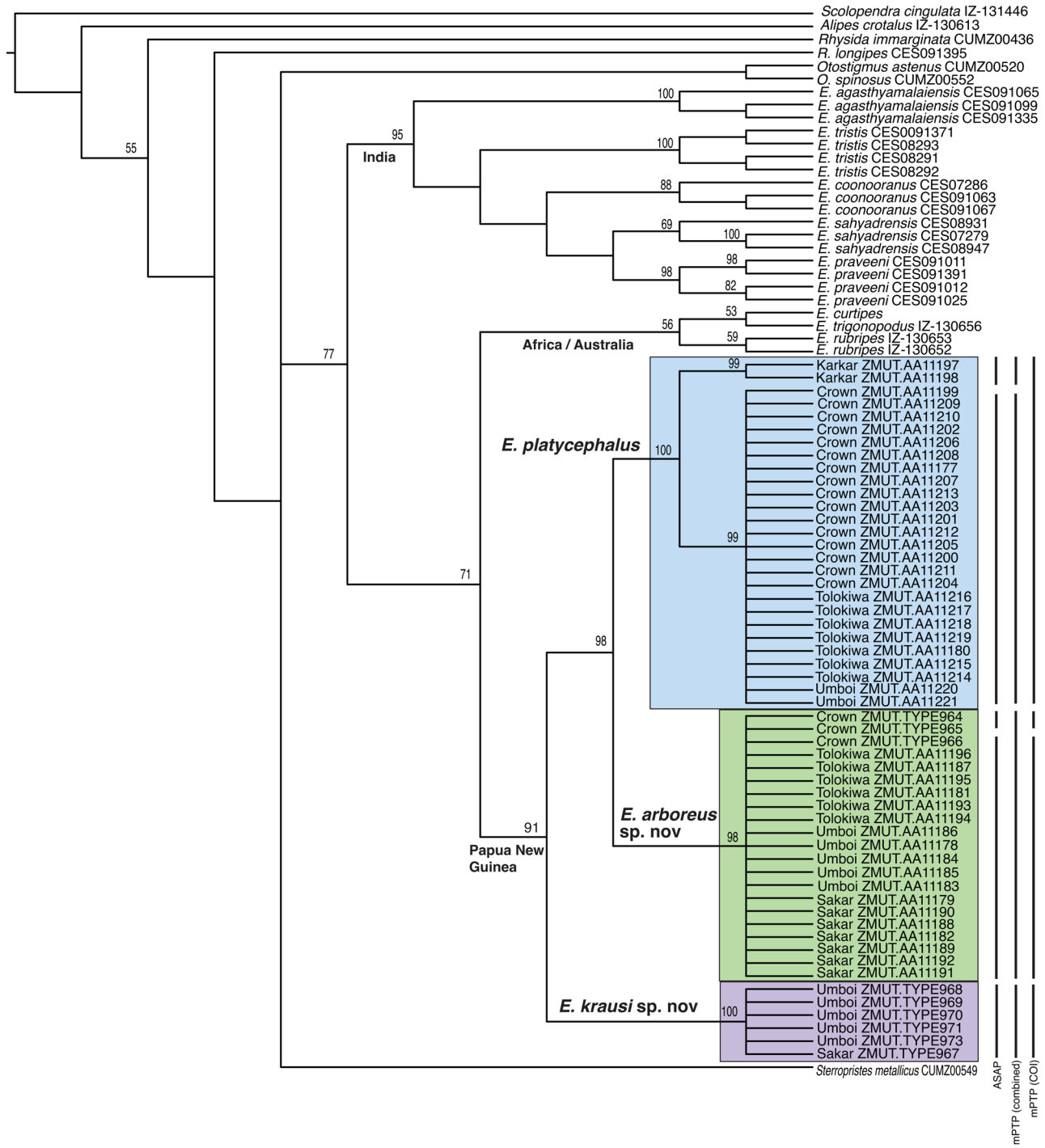

Fig. 10. Strict consensus of 5736 trees of length 2474 steps based on COI, 16S and 28S sequence data. Numbers at nodes are jackknife support values. Bars at the right margin show the species delimitations by ASAP and mPTP.

Ecology

A clear partitioning of habitat use between 2 of the species was evident during collection of the specimens. All individuals ($n = 25$) of *E. platycephalus* were collected as bycatch in bucket traps on the forest floor or while digging through rotten logs. In contrast, all individuals of *E. arboreus* ($n = 22$) were either caught from trees at night or while dissecting the leaf axils and masses of dead leaves of standing pandanus trees during the day. In no case were they obtained from the ground.

We were unable to gather reliable habitat data for *E. krausi* as the number of collected specimens was relatively low ($n = 10$) and most were brought to us by locals employed to collect on Sakar and Umboi.

Discussion

At least 2 of the species showed clearly distinct use of habitats, *E. platycephalus* being ground-dwelling and *E. arboreus* being arboreal. *Ethmostigmus arboreus* has significantly longer limbs

(12.3% in LP6 and 15.0% in LP 20) than *E. platycephalus*. The proportions of the different limb articles also differ between the 2 species, with the largest differences found in the prefemur (19.4% in LP6 and 21.1% in LP20) and the smallest differences in tarsus 2 (3.7% in LP6 and 2.6% in LP20).

While ecological data are missing for *E. krausi*, it is interesting to note that the largest differences in article proportions between that and *E. arboreus* are found in the prefemur (17.9% [LP6] and 17.5% [LP20] longer in *E. arboreus*). In contrast, the largest difference between *E. krausi* and *E. platycephalus* is found in tarsus 1 and 2 (tarsus 2 is 8.2% longer in *E. krausi* in LP6 and tarsus 1 is 13.0% longer in LP20). The total limb length in *E. krausi* is intermediate to that of *E. arboreus* and *E. platycephalus*, possibly pointing to a more generalized ecology or adaptation to a different microhabitat altogether.

The question arises whether longer limbs represent a specific adaptation to arboreality. There are surprisingly few studies on the correlation of limb length and arboreality in arthropods. Ober (2003) found no evidence that adaptation to an arboreal lifestyle in carabid beetles resulted in longer limbs.

Most research on the correlation between limb length and lifestyle has been done in lizards, where arboreality is usually divided into at least 2 different niches: "trunk" and "crown/twig," each with its own ecomorphological adaptations. *Anolis*, *Tropidurus*, and *Draco* species adapted to living on tree trunks tend to have longer limbs, whereas those adapted to using thinner branches and twigs tend to have shorter limbs (Losos 1994, Kohlsdorf *et al.* 2001, Ord and Klomp 2014). In *Cyrtodactylus*, the longest legs are generally found in scansorial species living on tree trunks or rocks and cliffs when compared to terrestrial and crown-dwelling species (Riedel *et al.* 2024). A similar correlation between arboreality and longer limb length is found in skinks (Foster *et al.* 2018).

Longer limbs provide higher sprint speed (Garland and Losos 1994), which may be more important for species exposed on open surfaces, such as tree trunks, when compared to species living in more sheltered habitats such as leaf litter or canopy (Goodman *et al.* 2008).

Another possibility is that the terrestrial species has adapted to life in the leaf litter by a reduction in limb length. Limb reduction in lizards is associated with adaptations to "closed" habitats such as subterranean (sand, humus layer), grassland, or crevices where long limbs form an impediment to movement (Camaiti *et al.* 2021, 2023). One example would be skinks of the genus *Sphenomorphus*, which, during our fieldwork, were found to broadly share microhabitat with the *E. platycephalus* in the leaf litter and the crevices of rotten logs. Indeed, most specimens of this species of *Ethmostigmus* were found while searching for *Sphenomorphus* spp.

An impediment to understanding the correlation between microhabitat and limb length in centipedes is the lack of previous studies, resulting in a large gap in data, which makes it difficult to determine whether the limbs have become elongated in the arboreal species, reduced in the terrestrial species, or both. Here, it is notable that *E. krausi*, which is phylogenetically sister to *E. arboreus* and *E. platycephalus*, exhibits an intermediate limb length, possibly reflecting the ancestral state. With all 3 species being sympatric (at least on Umboi), however, it is possible that competition could have driven morphological evolution affecting limb length in *E. krausi* as well.

Our observation during fieldwork was that the population densities of giant centipedes were unusually high on the islands visited in the Bismarck volcanic arc (Crown, Tolokiwa, Sakar, and Umboi) compared to other regions in Papua New Guinea where we have worked. For example, efforts to collect *Ethmostigmus* during 2 weeks of fieldwork in Central Province (Varirata and the Port Moresby region) resulted in the capture of only a single specimen, whereas several animals were usually encountered during night surveys on the islands. Although total centipede densities appeared to be significantly lower on these mainland sites, the generic diversity of large centipedes was higher and included species of *Scolopendra* and *Rhysida* in addition to *Ethmostigmus*; both of these genera were absent from the Bismarck volcanic arc islands. The limited size of oceanic islands accompanied by dispersal barriers often lead to depauperate species assemblages (König *et al.* 2021). It is possible that the resident *Ethmostigmus* species have experienced release from more distantly related competitors and predators, which could have resulted in density compensation (higher population densities) (Diamond 1970). The intensified interspecific competition could then have driven character displacement and niche partitioning in a way not seen in mainland communities.

It is worth noting here that divergence dates for all Indian species of *Ethmostigmus* have been estimated to be Paleogene (Joshi and Edgecombe 2019). Comparison of between-species branch lengths for India and the Bismarck volcanic arc in our maximum-likelihood tree (Fig. 8) suggests that all 3 species in the latter region are likewise older than the islands themselves, which are estimated to be of Quaternary origin (Robinson and Jaques 1978). Hence, it is likely that all 3 species originated on New Guinea or one of the Paleo islands, which have accreted to form that island and subsequently colonized the islands of the volcanic arc in geologically recent time. Future work is clearly needed to better understand the distribution and diversity of centipedes in the New Guinea region.

Conclusions

Taxonomic interpretation of chilopod diversity in the New Guinea region has hitherto mainly relied on a limited number of historical collections and species descriptions dating back to the late 19th and early 20th centuries. The morphological conservatism and small number of informative characters make species identification and the understanding of species boundaries challenging, but the situation is assisted by an integrative taxonomic approach that includes molecular sequence data.

Our study, which integrated dense sampling of a limited geographical region, molecular data, and ecological observations, strongly indicates that the taxonomic and ecological diversity of *Ethmostigmus* (and potentially other chilopod genera) is underestimated. It also provides an interesting case of niche partitioning and ecomorphological divergence between closely related species of *Ethmostigmus*.

Specimen Collection Statement

Nagoya Protocol: The authors attest that all legal and regulatory requirements, including export and import collection permits, have been followed for the collection of specimens from source populations at any international, national, regional, or other geographic level for all relevant field specimens collected as part of this study.

Nomenclature

This paper and the nomenclatural acts it contains have been registered in Zoobank (www.zoobank.org), the official register of the International Commission on Zoological Nomenclature. The LSID (Life Science Identifier) number of the publication is: urn: lsid:zoobank.org:pub:89F02509-7EBA-40DF-B194-8D E2DCBD4FE1.

Acknowledgements

We thank the National Research Institute of Papua New Guinea for national permits and the local governments of Morobe and Madang for provincial permits to conduct this research. We also thank the communities on Karkar, Crown, Tolokiwa, Umboi, and Sakar islands for permission to stay and work on their land. Dr Ligia Benavides kindly provided photos of the types in the Museum of Comparative Zoology, Harvard University. Dr Hannco Bakker facilitated C.A.M.-M.'s visit to Naturalis Biodiversity Center, and Dr Peter Jäger kindly provided access to collections at the Senckenberg Research Institute and Natural History Museum, Frankfurt. Two anonymous reviewers provided constructive comments on the manuscript.

Author Contributions

Valter Weijola (Conceptualization [equal], Funding acquisition [lead], Investigation [lead], Writing—original draft [equal], Writing—review & editing [equal]), Greg Edgecombe (Investigation [equal], Methodology [equal], Writing—original draft [equal], Writing—review & editing [equal]), Carlos Martínez-Muñoz (Investigation [supporting], Validation [supporting], Writing—original draft [supporting]), Bulisa Iova (Investigation [supporting]), Conny Sjöqvist (Formal analysis [equal], Methodology [equal], Writing—original draft [supporting]), and Varpu Vahtera (Data curation [equal], Formal analysis [equal], Investigation [equal], Writing—original draft [equal], Writing—review & editing [equal])

Supplementary Material

Supplementary material is available at *Insect Systematics and Diversity* online.

Funding

Weijola's work was supported by grants 105541 and 158161 from the Swedish Cultural Foundation and grant 226R-17 from the National Geographic Society.. Molecular work was supported by Turku University Foundation and Entomologiska Föreningen i Helsingfors.

Conflicts of Interest

None declared.

Data Availability

Sequence data used in this study are all available via GenBank. Morphometric data are available in Supporting Information, File S1.

References

Attems C. 1897. Myriopoden. *Abh. Senckenb. Naturf. Ges.* 23:473–536.

Attems C. 1930. Myriapoda. 2. Scolopendromorpha. In: Schulze FE, Kükenthal W, editors. *Das Tierreich*. Walter de Gruyter. p. 308.

Benavides LR, Jiang C, Giribet G. 2021. Mimopidae is the sister group to all other scolopendromorph centipedes (Chilopoda, Scolopendromorpha): a phylotranscriptomic approach. *Org. Divers. Evol.* 21:591–598. https://doi.org/10.1007/s13127-021-00502-2

Brandt JF. 1840. Observations sur les espèces qui composent la genre *Scolopendra* suivies des caractères des espèces qui se trouvent dans le Museum zoologique de l'Académie des Sciences de St-Pétersbourg et de quelque coup d'oeil sur leur distribution géographique. *Bull. Sci. Acad. Imp. Sci. Saint Pétersbourg*. 7:148–160.

Brown WL, Wilson EO. 1956. Character displacement. *Syst. Zool.* 5:49–64.

Butler AG. 1877. On the Myriopoda obtained by the Rev. G. Brown in Duke-of-York Island. *Proc. Zool. Soc. Lond*. 1877:282–283.

Camaiti M, Evans AR, Hipsley CA, et al. 2021. A farewell to arms and legs: a review of limb reduction in squamates. *Biol. Rev. Camb. Philos. Soc*. 96:1035–1050. https://doi.org/10.1111/brv.12690

Camaiti M, Evans AR, Hipsley CA, et al. 2023. Macroecological and biogeographical patterns of limb reduction in the world's skinks. *J. Biogeogr*. 50:428–440. https://doi.org/10.1111/jbi.14547

Cámara-Leret R, Frodin DG, Adema F, et al. 2020. New Guinea has the world's richest island flora. *Nature*. 584:579–583. https://doi.org/10.1038/s41586-020-2549-5

Chamberlin RV. 1920. The Myriopoda of the Australian region. *Bull. Mus. Comp. Zool. Harv*. 64:1–269.

Chamberlin RV. 1939. On a collection of chilopods from the East Indies. *Bull. Univ. Utah Biol. Ser*. 29:1–19.

Chamberlin RV. 1944. Some chilopods from the Indo-Australian archipelago. *Notulae Naturae*. 147:1–14.

Darwin C. 1845. *Journal of researches into the natural history and geology of the countries visited during the voyage of H.M.S. Beagle Round the World*. 2nd ed. John Murray.

Darwin C. 1859. *On the origin of species*. John Murray.

Diamond JM. 1970. Ecological consequences of island colonization by southwest Pacific birds, I. Types of niche shifts. *Proc. Natl. Acad. Sci. U S A*. 67:529–536.

Diamond J, Pimm SL, Gilpin ME, et al. 1989. Rapid evolution of character displacement in myzomelid honeyeaters. *Am. Nat*. 134:675–708.

Duffels JP. 1986. Biogeography of Indo-Pacific Cicadoidea: a tentative recognition of areas of endemism. *Cladistics*. 2:318–336.

Edgecombe GD, Giribet G. 2004. Adding mitochondrial sequence data (16S rRNA and cytochrome *c* oxidase subunit I) to the phylogeny of centipedes (Myriapoda: Chilopoda): an analysis of morphology and four molecular loci. *J. Zoological System*. 42:89–134. https://doi.org/10.1111/j.1439-0469.2004.00245.x

Edgecombe GD, Giribet G, Wheeler WC. 2002. Phylogeny of Henicopidae (Chilopoda: Lithobiomorpha): a combined analysis of morphology and five molecular loci. *Syst. Entomol*. 27:31–64. https://doi.org/10.1046/j.0307-6970.2001.00163.x

Edgecombe GD. 2011. Chilopoda—fossil history. In: Minelli A, editor. *Treatise on zoology—anatomy, taxonomy, biology. The Myriapoda*. Vol. 1. Brill, Leiden. p. 355–361.

Edgecombe GD, Bonato L. 2011. Chilopoda—taxonomic overview. Order Scolopendromorpha. In: Minelli A, editor. *Treatise on zoology—anatomy, taxonomy, biology. The Myriapoda*. Vol. 1. Brill, Leiden. p. 392–407.

Farris JS, Albert VA, Källersjö M, et al. 1996. Parsimony jackknifing outperforms neighbor joining. *Cladistics*. 12:99–124. https://doi.org/10.1006/clad.1996.0008

Folmer O, Black M, Hoeh W, et al. 1994. DNA primers for amplification of mitochondrial cytochrome c oxidase subunit I from diverse metazoan invertebrates. *Mol. Mar. Biol. Biotechnol*. 3:294–299.

Foster KL, Garland TJr, Schmitz L, et al. 2018. Skink ecomorphology: forelimb and hind limb lengths, but not static stability, correlate with

habitat use and demonstrate multiple solutions. *Biol. J. Linn. Soc.* 125:673–692. https://doi.org/10.1093/biolinnean/bly146
Fox J, Weisberg S. 2019. *An R companion to applied regression*. 3rd ed. Sage.
Garland TJr, Losos JB. 1994. Ecological morphology of locomotor performance in squamate reptiles. In: Wainwright PC, Reilly SM, editors. *Ecological morphology: integrative organismal biology*. The University of Chicago Press. p. 240–302.
Gillespie RG, Roderick GK. 2002. Arthropods on islands: colonization, speciation, and conservation. *Annu. Rev. Entomol.* 47:595–632. https://doi.org/10.1146/annurev.ento.47.091201.145244
Giribet G, Carranza S, Riutort M, et al. 1999. Internal phylogeny of the Chilopoda (Myriapoda: Arthropoda) using complete 18S rDNA and partial 28S rDNA sequences. *Philos. Trans. R Soc. Lond. B Biol. Sci.* 354:215–222. https://doi.org/10.1098/rstb.1999.0373
Giribet G, Edgecombe GD, Wheeler WC. 2001. Arthropod phylogeny based on eight molecular loci and morphology. *Nature* 413:157–161. https://doi.org/10.1038/35093097
Goloboff PA. 1999. Analyzing large data sets in reasonable times: solutions for composite optima. *Cladistics* 15:415–428. https://doi.org/10.1006/clad.1999.0122
Goloboff PA, Catalano SA. 2016. TNT version 1.5, including a full implementation of phylogenetic morphometrics. *Cladistics* 32:221–238. https://doi.org/10.1111/cla.12160
Goodman BA, Miles DB, Schwarzkopf L. 2008. Life on the rocks: habitat use drives morphological and performance evolution in lizards. *Ecology* 89:3462–3471. https://doi.org/10.1890/07-2093.1
Grant PR, Grant BR. 2008. *How and why species multiply: the radiation of Darwin's finches*. Princeton University Press. https://doi.org/10.1515/9781400837946
Haase E. 1887. Die Indisch-Australischen Myriopoden. I. Chilopoda. *Abh. Ber. Königl. Zool. Anthropol.-Ethnogr. Mus. Dresden* 5:1–118.
Hodges CW, Goodyear J. 2021. Novel foraging behaviors of *Scolopendra dehaani* (Chilopoda: Scolopendridae) in Nakhon Ratchasima, Thailand. *Int. J. Trop. Insect Sci.* 41:3257–3262. https://doi.org/10.1007/s42690-021-00431-9
Hothorn T, Bretz F, Westfall P. 2008. Simultaneous inference in general parametric models. *Biom. J.* 50:346–363. https://doi.org/10.1002/bimj.200810425
Humphries JM, Bookstein FL, Chernoff B, et al. 1981. Multivariate discrimination by shape in relation to size. *Syst. Zool.* 30:291–308.
Johnson RW, Taylor GAM, Davies RA. 1972. Geology and petrology of quaternary volcanic islands off the north coast of New Guinea. *Bur. Min. Res., Geol. Geophys. Rec.* 21:127.
Joshi J, Edgecombe GD. 2018. Molecular phylogeny and systematics of the centipede genus *Ethmostigmus* Pocock (Chilopoda: Scolopendromorpha) from peninsular India. *Invert. Syst.* 32:1316–1335. https://doi.org/10.1071/IS18030
Joshi J, Edgecombe GD. 2019. Evolutionary biogeography of the centipede genus *Ethmostigmus* from peninsular India: testing an ancient vicariance hypothesis for Old World tropical diversity. *BMC Evol. Biol.* 19:41. https://doi.org/10.1186/s12862-019-1367-6
Joshi J, Karanth PK, Edgecombe GD. 2020. The Out-of-India hypothesis: evidence from an ancient centipede genus, *Rhysida* (Chilopoda: Scolopendromorpha) from the Oriental Region, and systematics of Indian species. *Zool. J. Linn. Soc.* 189:828–861. https://doi.org/10.1093/zoolinnean/zlz138
Kapli P, Lutteropp S, Zhang J, et al. 2017. Multi-rate Poisson tree processes for single-locus species delimitation under maximum likelihood and Markov chain Monte Carlo. *Bioinformatics*. 33:1630–1638. https://doi.org/10.1093/bioinformatics/btx025
Katoh K, Rozewicki J, Yamada KD. 2019. MAFFT online service: multiple sequence alignment, interactive sequence choice and visualization. *Brief. Bioinform.* 20:1160–1166. https://doi.org/10.1093/bib/bbx108
Koch LE. 1983. A taxonomic study of the centipede genus *Ethmostigmus* Pocock (Chilopoda: Scolopendridae: Otostigminae) in Australia. *Aust. J. Zool.* 31:835–849.
Kohlsdorf T, Garland TJr, Navas CA. 2001. Limb and tail lengths in relation to substrate usage in *Tropidurus* lizards. *J. Morphol.* 248:151–164. https://doi.org/10.1002/jmor.1026
König C, Weigelt P, Taylor A, et al. 2021. Source pools and disharmony of the world's island floras. *Ecography*. 44:44–55. https://doi.org/10.1111/ecog.05174
Kraus F, Vahtera V, Weijola V. 2023. A new species of *Lepidodactylus* (Squamata: Gekkonidae) from Umboi Island, Papua New Guinea. *Zootaxa*. 5296:525–539. https://doi.org/10.11646/zootaxa.5296.4.2
Kraus F, Vahtera V, Weijola V. 2024. A new species of insular *Gehyra* (Squamata; Gekkonidae) from Papua New Guinea closely related to *Gehyra oceanica*. *Syst. Biodivers* 22. https://doi.org/10.1080/14772000.2024.2404829
Kraus F, Weijola V. 2019. New species of *Cyrtodactylus* (Squamata: Gekkonidae) from Karkar Island, Papua New Guinea. *Zootaxa*. 4695:zootaxa.4695.6.3. https://doi.org/10.11646/zootaxa.4695.6.3
Kronmüller C. 2009. A new species of Scolopender from the Philippines (Chilopoda: Scolopendridae). *Arthropoda*. 17:48–51.
Kuraku S, Zmasek CM, Nishimura O, et al. 2013. aLeaves facilitates on-demand exploration of metazoan gene family trees on MAFFT sequence alignment server with enhanced interactivity. *Nucleic Acids Res*. 41:W22–W28. https://doi.org/10.1093/nar/gkt389
Lewis JGE. 1972. The life histories and distribution of the centipede *Rhysida nuda togoensis* and *Ethmostigmus trigonopodus* (Scolopendromorpha: Scolopendridae) in Nigeria. *J. Zool.* 167:399–414.
Losos JB. 1994. Integrative approaches to evolutionary ecology: *Anolis* lizards as model systems. *Annu. Rev. Ecol. Syst.* 25:467–493.
Maddison WP, Maddison DR. 2019. Mesquite: a modular system for evolutionary analysis. Version 3. http://www.mesquiteproject.org
Miller MA, Pfeiffer W, Schwartz T. 2010. Creating the CIPRES Science Gateway for inference of large phylogenetic trees. In GatewayComputing Environments Workshop (GCE), New Orleans, LA, USA.pp. 1-8. https://doi.org/10.1109/GCE.2010.5676129
Murienne J, Edgecombe GD, Giribet G. 2010. Including secondary structure, fossils and molecular dating in the centipede tree of life. *Mol. Phylogenet. Evol.* 57:301–313. https://doi.org/10.1016/j.ympev.2010.06.022
Newport G. 1845. Monograph of the class Myriapoda order Chilopoda; with observations of the general arrangement of the Articulata. *Trans. Linn. Soc. Lond*. 19:265–302.
Ober KA. 2003. Arboreality and morphological evolution in ground beetles (Carabidae: Harpalinae): testing the taxon pulse model. *Evolution* 57:1343–1358. https://doi.org/10.1111/j.0014-3820.2003.tb00342.x
Oliver PM, Bower DS, McDonald PJ, et al. 2022. Melanesia holds the world's most diverse and intact insular amphibian fauna. *Commun. Biol.* 5:1182. https://doi.org/10.1038/s42003-022-04105-1
Oliver PM, Kraus F, Austin J, et al. 2024. Lineage diversity in a Melanesian lizard radiation (Gekkonidae: *Nactus*) further highlights exceptional diversity and endemism in eastern Papua New Guinea. *Org. Divers. Evol.* 24:557–572. https://doi.org/10.1007/s13127-024-00655-w
Ord TJ, Klomp DA. 2014. Habitat partitioning and morphological differentiation: the Southeast Asian *Draco* lizards and Caribbean *Anolis* lizards compared. *Oecologia*. 175:651–666. https://doi.org/10.1007/s00442-014-2921-y
Pérez-Delgado AJ, Arribas P, Hernando C, et al. 2022. Hidden island endemic species and their implications for cryptic speciation within soil arthropods. *J. Biogeogr*. 49:1367–1380. https://doi.org/10.1111/jbi.14388
Phillips JW, Chung AYC, Edgecombe GD, et al. 2020. Bird's nest ferns promote resource sharing by centipedes. *Biotropica*. 52:335–344. https://doi.org/10.1111/btp.12713
Pocock RI. 1899. Report on the centipedes and millipedes obtained by Dr A. Willey in the Loyalty Islands, New Britain, and elsewhere. In: Willey A, editor. *Zoological results based on material from New Britain, New Guinea, Loyalty Islands and elsewhere*. Cambridge University Press. Vol. 1. p.59–74.
Polhemus DA, Allen GR, Englund RA. 2004. *Freshwater biotas of New Guinea and nearby islands: an analysis of endemism, richness, and threats*. Vol. 31. Bishop Museum.

Price TD. 2008. *Speciation in birds*. Roberts and Company. https://doi.org/10.1525/cond.2008.8620

Puillandre N, Brouillet S, Achaz G. 2021. ASAP: assemble species by automatic partitioning. *Mol. Ecol. Resour*. 21:609–620. https://doi.org/10.1111/1755-0998.13281

R Core Team. 2021. *R: a language and environment for statistical computing*. R Foundation for Statistical Computing. http://www.R-project.org/

Riedel J, Grismer LL, Higham T, et al. 2024. Ecomorphology of the locomotor apparatus in the genus *Cyrtodactylus* (Gekkota, Squamata). *Evol. Biol*. 51:106–123. https://doi.org/10.1007/s11692-023-09622-3

Robinson GP, Jaques AL. 1978. Karkar Island, Papua New Guinea—1:250,000 Geological Series. Explanatory notes to accompany Karkar Island 1:250,000 geological map. Geological Survey of Papua New Guinea, Explanatory Notes. SB/55–52.

RStudio Team. 2021. *RStudio: integrated development environment for R*. RStudio, PBC. http://www.rstudio.com/

Schileyko AA, Stagl V. 2004. The collection of scolopendromorph centipedes (Chilopoda) in the Natural History Museum in Vienna: a critical re-evaluation of former taxonomic identifications. *Ann. Naturhist. Mus. Wien*. 105:B:67–137.

Schileyko AA, Stoev PE. 2016. Scolopendromorpha of New Guinea and adjacent islands (Myriapoda, Chilopoda). *Zootaxa*. 4147:247–280. https://doi.org/10.11646/zootaxa.4147.3.3

Schileyko AA, Vahtera V, Edgecombe GD. 2020. An overview of the extant genera and subgenera of the order Scolopendromorpha (Chilopoda): a new identification key and updated diagnoses. *Zootaxa*. 4825:zootaxa.4825.1.1. https://doi.org/10.11646/zootaxa.4825.1.1

Siriwut W, Edgecombe GD, Sutcharit C, et al. 2015. The centipede genus *Scolopendra* in mainland Southeast Asia: molecular phylogenetics, geometric morphometrics and external morphology as tools for species delimitation. *PLoS One*. 10:e0135355. https://doi.org/10.1371/journal.pone.0135355

Siriwut W, Edgecombe GD, Sutcharit C, et al. 2016. A taxonomic review of the centipede genus *Scolopendra* Linnaeus, 1758 (Scolopendromorpha, Scolopendridae) in mainland Southeast Asia, with description of a new species from Laos. *Zookeys*. 590:1–124. https://doi.org/10.3897/zookeys.590.7950

Siriwut W, Edgecombe GD, Sutcharit C, et al. 2018. Systematic revision and phylogenetic reassessment of the centipede genera *Rhysida* Wood, 1862 and *Alluropus* Silvestri, 1912 (Chilopoda: Scolopendromorpha) in Southeast Asia, with further discussion of the subfamily Otostigminae. *Invert. Syst*. 32:1005–1049. https://doi.org/10.1071/IS17081

Slavenko A, Allison A, Austin J, et al. 2023. Skinks of Oceania, New Guinea, and Eastern Wallacea: an underexplored biodiversity hotspot. *Pac. Conserv. Biol*. 29:526–543. https://doi.org/10.1071/PC22034

Stamatakis A. 2014. RAxML Version 8: a tool for phylogenetic analysis and post-analysis of large phylogenies. *Bioinformatics*. 30:1312–1313. https://doi.org/10.1093/bioinformatics/btu033

Stamatakis A, Hoover P, Rougemont J. 2008. A rapid bootstrap algorithm for the RAxML Web servers. *Syst. Biol*. 57:758–771. https://doi.org/10.1080/10635150802429642

Tsukamoto S, Hiruta SF, Eguchi K, et al. 2021. A new amphibious species of the genus *Scolopendra* Linnaeus, 1758 (Scolopendromorpha, Scolopendridae) from the Ryukyu Archipelago and Taiwan. *Zootaxa*. 4952:zootaxa.4952.3.3. https://doi.org/10.11646/zootaxa.4952.3.3

Vahtera V, Edgecombe GD, Giribet G. 2012. Evolution of blindness in scolopendromorph centipedes (Chilopoda: Scolopendromorpha): insights from an expanded sampling of molecular data. *Cladistics*. 28:4–20. https://doi.org/10.1111/j.1096-0031.2011.00361.x

Vahtera V, Edgecombe GD, Giribet G. 2013. Phylogenetics of scolopendromorph centipedes: can denser taxon sampling improve an artificial classification? *Invert. Syst*. 27:578–602. https://doi.org/10.1071/IS13035

Vaidya G, Lohman DJ, Meier R. 2011. SequenceMatrix: concatenation software for the fast assembly of multi-gene datasets with character set and codon information. *Cladistics*. 27:171–180. https://doi.org/10.1111/j.1096-0031.2010.00329.x

Voigtländer K. 2011. Chilopoda—Ecology. In: Minelli A, editor. *Treatise on zoology—anatomy, taxonomy, biology. The Myriapoda*. Vol. 1. Brill, Leiden. p. 309–325.

Wallace AR. 1880. *Island life: or, the phenomena and causes of insular faunas and floras, including a revision and attempted solution of the problem of geological climate*. Macmillan and Co.

Whiting MF, Carpenter JM, Wheeler QD, et al. 1997. The Strepsiptera problem: phylogeny of the holometabolous insect orders inferred from 18S and 28S ribosomal DNA sequences and morphology. *Syst. Biol*. 46:1–68. https://doi.org/10.1093/sysbio/46.1.1

Wickham H. 2016. *ggplot2: elegant graphics for data analysis*. 2nd ed. Springer Int. Publ.

Wilson EO. 1961. The nature of the taxon cycle in the Melanesian ant fauna. *Am. Nat*. 95:169–193.

Xiong B, Kocher TD. 1991. Comparison of mitochondrial DNA sequences of seven morphospecies of black flies (Diptera: Simuliidae). *Genome*. 34:306–311.